Journal of Medicinal Chemistry

pubs.acs.org/jmc

Article

Positron Emission Tomography Imaging of Neurotensin Receptor-Positive Tumors with ^{68}Ga-Labeled Antagonists: The Chelate Makes the Difference Again

Emma Renard, Mathieu Moreau, Pierre-Simon Bellaye, Mélanie Guillemin, Bertrand Collin, Aurélie Prignon, Franck Denat, and Victor Goncalves*

Cite This: *J. Med. Chem.* 2021, 64, 8564−8578

Read Online

ACCESS | Metrics & More | Article Recommendations | Supporting Information

ABSTRACT: Neurotensin receptor 1 (NTS_1) is involved in the development and progression of numerous cancers, which makes it an interesting target for the development of diagnostic and therapeutic agents. A small molecule NTS_1 antagonist, named [^{177}Lu]Lu-IPN01087, is currently evaluated in phase I/II clinical trials for the targeted therapy of neurotensin receptor-positive cancers. In this study, we synthesized seven compounds based on the structure of NTS_1 antagonists, bearing different chelating agents, and radiolabeled them with gallium-68 for PET imaging. These compounds were evaluated *in vitro* and *in vivo* in mice bearing a HT-29 xenograft. The compound [^{68}Ga]Ga-bisNODAGA-**16** showed a promising biodistribution profile with mainly signal in tumor (4.917 ± 0.776%ID/g, 2 h post-injection). Its rapid clearance from healthy tissues led to high tumor-to-organ ratios, resulting in highly contrasted PET images. These results were confirmed on subcutaneous xenografts of AsPC-1 tumor cells, a model of NTS_1-positive human pancreatic adenocarcinoma.

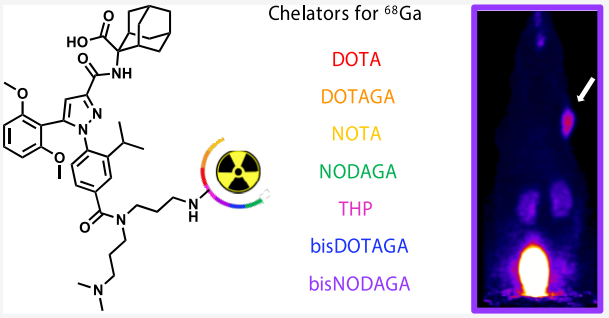

INTRODUCTION

Molecular imaging is a non-invasive technique that participates to the rapid and accurate diagnosis of many cancers. It relies on the administration of an imaging probe capable of binding specifically to a biomarker of the disease. The localization of this probe is then classically achieved by positron emission tomography (PET) or single photon emission computed tomography (SPECT) in oncology.[1]

An interesting target involved in the development and progression of numerous cancers is the neurotensin receptor 1 (NTS_1).[2,3] This G-protein coupled receptor is overexpressed in different cancers such as pancreatic ductal adenocarcinoma,[4] prostate cancer,[5] Ewing's sarcoma,[6] colorectal cancer,[7] breast cancer,[8] and small cell lung cancer, but not present in healthy tissues.[9] The endogenous ligand of this receptor is a tridecapeptide called neurotensin (NT).[10]

These last years, neurotensin and its receptors have been the subject of numerous studies. Most of them deal with the design of NTS_1 agonists. Those agonists are generally peptide analogs of neurotensin, which have been labeled with radiometals or fluorophores for nuclear imaging, radiotherapy, or fluorescence imaging.[11−14] Despite their good affinity for NTS_1 (in the nanomolar range) and interesting biodistribution properties, these compounds often present limited metabolic stability, even after chemical optimization.[15,16]

In the early 90s, Sanofi-Recherche discovered a nonpeptidic antagonist of NTS_1 named SR45398 (Figure 1).[17,18] After a few years of optimization, they identified SR142948A, a drug candidate with nanomolar affinity and potency for neurotensin receptors.[19,20] Starting from the structure of SR142948A, a few radiotracers were developed for the diagnosis or therapy of neurotensin receptor-positive cancers. Such tracers present several advantages: in the absence of activation of receptor's signaling pathways, they produce no pharmacological effect; they often show better metabolic stability than peptides,[21,22] and their small size allows for a rapid biodistribution, with fast renal clearance.

Furthermore, it has been shown that agonists and antagonists may not necessarily recognize the same conformational states of their receptors.[23−25] This phenomenon has also been observed with neurotensin receptors, by Betancur *et al.*, who showed that the number of receptors labeled by the antagonist [^{3}H]-SR142948A on rat brain membranes was 80% greater than that detected when using the agonist [^{3}H]neurotensin.[20]

In 2013, Lang *et al.* synthesized an analog of SR142948A and coupled it to 2-deoxy-2-[^{18}F]fluoroglucosylazide to create a PET

Received: March 22, 2021
Published: June 9, 2021

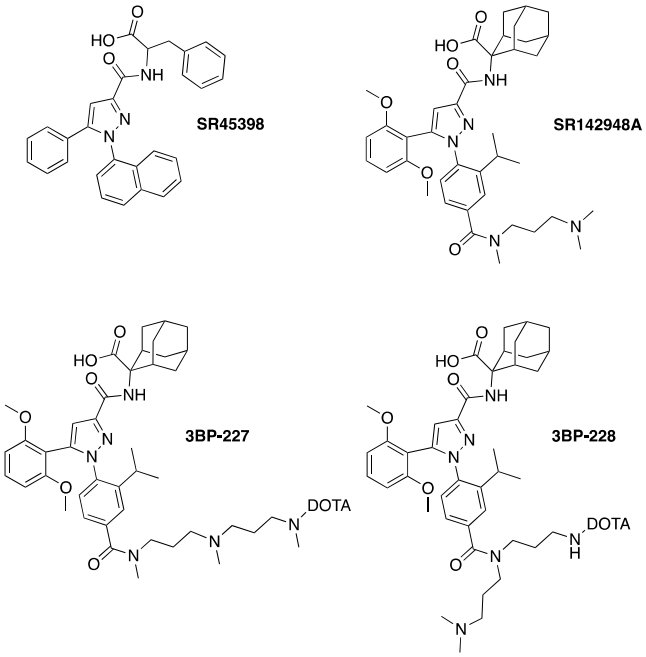

Figure 1. Chemical structures of SR45398, SR142948A, 3BP-227, and 3BP-228. DOTA stands for 1,4,7,10-tetraazacyclododecane-1,4,7,10-tetraacetic acid.

imaging tracer.[21] This compound showed an excellent affinity for NTS_1 (0.98 nM). However, despite a fairly good uptake in tumor tissues, a significant accumulation was observed in other organs, particularly the liver. In 2016, Schulz *et al.* introduced a polyazamacrocyclic metal-chelating agent (DOTA) on different analogs of SR142948A and radiolabeled them with indium-111, a radionuclide suitable for SPECT imaging.[26] Their compounds [^{111}In]In-3BP-227 and [^{111}In]In-3BP-228 (Figure 1) showed good affinity for neurotensin receptor 1 and high and specific tumor uptake *in vivo*. Because of its prolonged retention in the target tissue at late time-points (24 h after injection), 3BP-227 was considered as a good candidate for the radiotherapy of cancer. In 2017, Schulz *et al.*, evaluated 3BP-227 (now IPN01087) for the ^{177}Lu-radiotherapy of colon carcinoma in a preclinical study. Their promising results paved the way for a radiotherapy trial,[22] which was initiated in 2018 by Baum and coll. on patients with metastatic or locally advanced cancers expressing NTS_1.[27] Preliminary results provided clinical evidence of the feasibility of treatment of ductal pancreatic adenocarcinoma with the ^{177}Lu-labeled NTS_1 antagonist 3BP-227.[28]

The availability of a PET companion diagnostic agent would greatly facilitate the selection of patients eligible for NTS_1-targeted radiotherapy.[29] In this study, we sought to assess the influence of the chelator on the biodistribution of neurotensin receptor antagonists. A variety of chelating agents, suitable for the complexation of ^{68}Ga, was coupled to an analog of SR142948A. The resulting tracers were then evaluated *in vitro* and tested *in vivo* on mice xenografted with an HT-29 model of colorectal cancer or an AsPC-1 model of pancreatic cancer.

RESULTS AND DISCUSSION

Design and Synthesis. A series of seven imaging agents, antagonists of neurotensin receptors, were synthesized. In light of the study by Schulz *et al.*, we chose to build our compounds based on the structure of the compound 3BP-228.[26] This compound differs from 3BP-227 in its amine arm. Indeed, 3BP-227 carries a linear amine arm, whereas 3BP-228 has a branched amine arm (Figure 1). Tumor uptakes of [^{111}In]In-3BP-227 and [^{111}In]In-3BP-228 were similar at 3, 6, and 12 h post-injection, but tumor-to-normal tissue ratios were generally higher for [^{111}In]In-3BP-228 at the earliest time-point (3 h p.i.), although not statistically different. Since our objective was to design a PET tracer, showing rapid clearance from healthy tissues, in particular from the liver and gastrointestinal tract to facilitate the detection of the primary tumor and potential metastases, we felt that it was more interesting to select 3BP-228's scaffold. Nonetheless, the compound 3BP-227 was also synthesized and used as a reference in this study.

Gallium-68 was chosen as the radiometal. Indeed, this positron-emitting radioisotope has a short half-life of 67.7 min, which is perfectly suited to the rapid pharmacokinetics of small molecules and reduces patient exposure to ionizing radiation compared to other radiometals with longer half-lives such as copper-64 or zirconium-89. In addition, ^{68}Ga has a relatively low cost and is readily available thanks to ^{68}Ge/^{68}Ga generators.[30] Alternatively, it can be produced in cyclotrons *via* the ^{68}Zn(p,n)^{68}Ga reaction, which further increases the availability of this radiometal.[31]

Several chelating agents suitable for ^{68}Ga complexation are available.[32−34] Among them, we first chose to evaluate NOTA, (*R*)-NODAGA, DOTA, DOTAGA, and THP. All these chelators are able to form stable complexes. Due to their differences in charge and log*D*, we hypothesized that the presence of these chelates could significantly modify the pharmacokinetics of the tracers.[35−40] In addition, we have also chosen to introduce two (*R*)-NODAGA or DOTAGA chelators on the same molecule in order to increase clearance from blood and improve tumor-to-background ratios. This approach was inspired by the work of Roxin *et al.*, who showed that the introduction of a metal-free DOTA on a ^{18}F radiotracer could improve tumor uptake and increase renal excretion.[41]

The compounds were prepared by multi-step synthesis from four synthons (Scheme 1). The first synthon (**A**), 3-isopropyl-4-hydrazinobenzoic acid hydrochloride, was synthesized in six steps starting from 2-isopropylaniline with a yield of 9%.[42] The second synthon (**B**), ethyl-4-(2,6-dimethoxyphenyl)-4-hydroxy-2-oxobut-3-enoate was prepared, starting from diethyl oxalate and 2,6-dimethoxyacetophenone, with a yield of 73%.[43] The amine arm (synthon **C**) was obtained in three steps with a yield of 50%.[44] The fourth synthon (**D**), *tert*-butyl-2-aminoadamantane-2-carboxylate, was synthesized in four steps starting from 2-adamantanone with a yield of 23%.[45,46] The linear amine arm (synthon **E**), for the reference compound 3BP-227, was prepared in one step in 80% yield. Four steps were then required to obtain the precursor **16**, ready for conjugation with the different chelating agents.[42,47] Finally, the introduction of the chelators was achieved in one or two steps, in yields ranging from 15 to 65%.

Stability. In order to evaluate the stability of these molecules against enzymatic degradation, each compound was metalated with non-radioactive gallium and incubated in mouse serum at 37 °C. RP-HPLC-MS analyses were performed at different time-points (0 min, 30 min, 1 h, 2 h, 4 h, and 24 h). Interestingly, NOTA/NODAGA/THP-based compounds proved to be stable in these assay conditions (>99% intact product after 4 h) whereas DOTA/DOTAGA-based compounds showed some degradation (*ca.* 80% intact product after 4 h) (Table 1 and Table S1). The main degradation corresponded to the loss of

https://doi.org/10.1021/acs.jmedchem.1c00523
J. Med. Chem. 2021, 64, 8564−8578

Scheme 1. Synthesis of NTS_1 Antagonists[a]

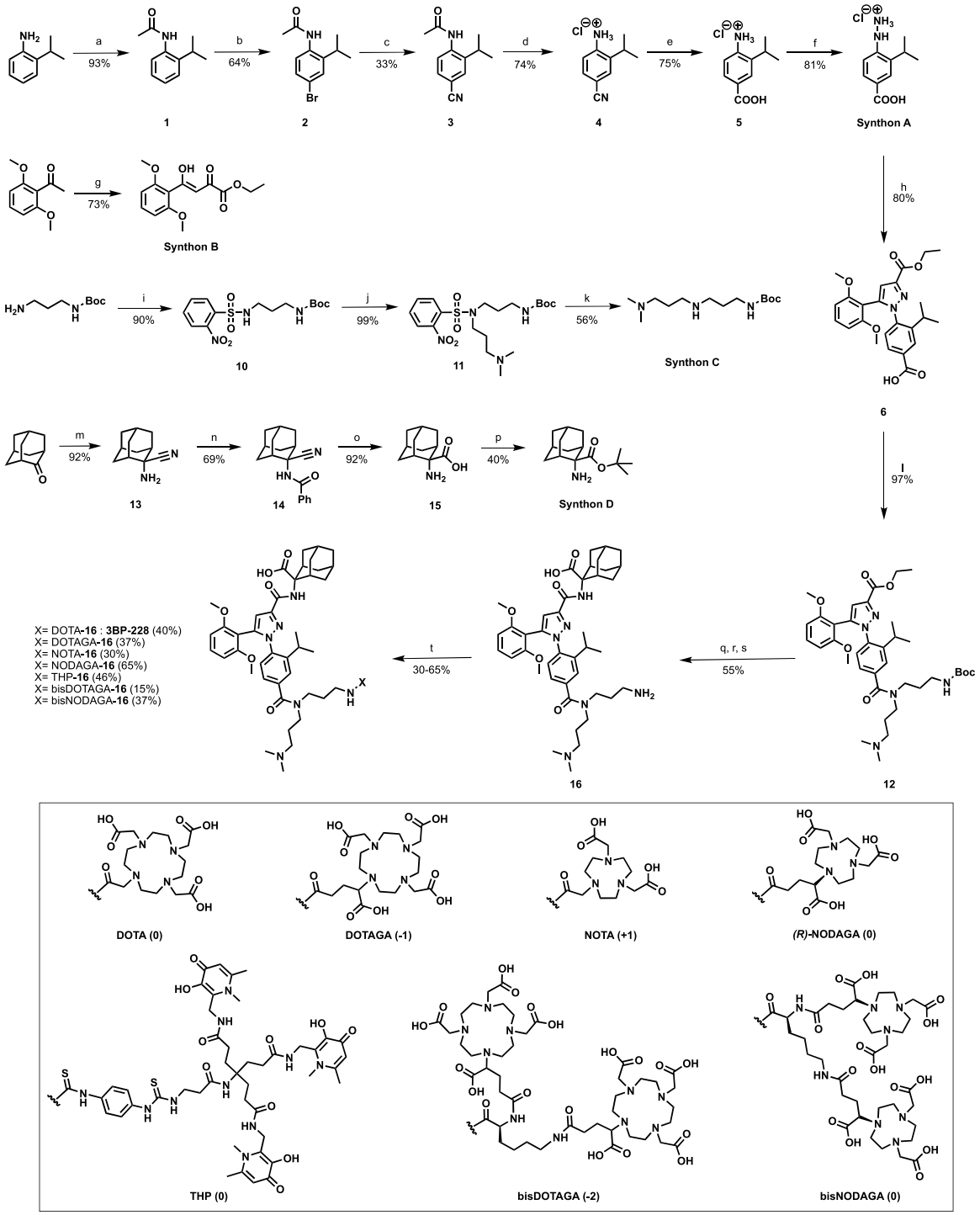

[a]Reagents and conditions: (a) Ac_2O, toluene, 0 °C to RT, 1 h; (b) NBS, DMF, RT, o.n.; (c) CuCN, H_2O/DMF, reflux, o.n.; (d) 1 M HCl, EtOH, reflux, 3 d; (e) KOH, 1,2-dimethoxyethane, reflux, 3 d; (f) (1) $NaNO_2$, HCl/AcOH, 0 °C, 3 h, (2) $SnCl_2$, HCl, RT, 2 h; (g) diethyl oxalate, NaH, DMF, RT, o.n.; (h) Synthon **B**, AcOH, reflux, 4 d; (i) 2-nitrobenzenesulfonyl chloride, NEt_3, CH_2Cl_2, 0 °C to RT, 15 min; (j) 3-dimethylamino-1-propyl hydrochloride, K_2CO_3, DMF, 60 °C, o.n.; (k) PhSH, Cs_2CO_3, DMF, 40 °C, 5 h; (l) Synthon **C**, HATU, DIPEA, DMF, RT, 6 h; (m) NaCN, NH_4OH, NH_4Cl, H_2O/EtOH, 50 °C, o.n.; (n) BzCl, K_2CO_3, H_2O/THF, RT, 2 h; (o) HCl/AcOH, reflux, 5 d; (p) *t*-butyl acetate, $HClO_4$, RT, o.n.; (q) KOH 5 M, dioxane, RT, 18 h.; (r) Synthon **D**, HATU, NEt_3, DMF, RT, 4 h; (s) TFA/DCM 50/50, RT, 1.5 h; (t) chelating agent, DIPEA, DMF, RT, 4 h. The values noted in parentheses are the estimated charge when each chelator is complexed to Ga^{3+} at pH 7.4.

gallium as evidenced by mass spectrometry. This shows the importance of the cavity size on the thermodynamic stability of ^{68}Ga complexes (the expansion of the macrocyclic ring results in a decrease in the complexation constant: $\log K_{Ga\text{-}NOTA}$ = 31.0 vs $\log K_{Ga\text{-}DOTA}$ = 26.1).[48] After 24 h, some unidentified degradation products (mass loss of 27) were also observed. Although these *in vitro* data do not necessarily reflect the metabolic stability of the compounds *in vivo*, they do confirm the

https://doi.org/10.1021/acs.jmedchem.1c00523
J. Med. Chem. 2021, 64, 8564−8578

Table 1. Percentage of Inhibition Constants, Intact Compound after 4 h, Partition Coefficients, and Radiochemical Purities of Compounds Tested in This Study

compound	Ki (nM)[a]	% intact after 4 h[b]	Log*D*[c]	Radiochemical purity (radio-HPLC)
[$^{nat/68}$Ga]Ga-3BP-228	1.35 [0.99−1.83]	80%	−2.45	>99%
[$^{nat/68}$Ga]Ga-DOTAGA-**16**	3.59 [3.03−4.26]	78%	−1.75	>99%
[$^{nat/68}$Ga]Ga-NOTA-**16**	0.73 [0.60−0.88]	> 99%	−1.85	94%
[$^{nat/68}$Ga]Ga-NODAGA-**16**	1.75 [0.77−3.96]	> 99%	−1.74	97%
[$^{nat/68}$Ga]Ga-THP-**16**	1.80 [1.55−2.10]	90%	−1.17	99%
[$^{nat/68}$Ga]Ga-bisDOTAGA-**16**	61.9 [51.9−73.8]	78%	−3.62	>99%
[$^{nat/68}$Ga]Ga-bisNODAGA-**16**	9.05 [7.28−11.2]	> 99%	−3.44	>99%
[$^{nat/68}$Ga]Ga-3BP-227	0.55 [0.51−0.59]	90%	−2.62	98%
[$^{nat/68}$Ga]Ga-DOTA-NT-20.3	10.0 [6.51−15.4]	N.D.	−2.50	>99%

[a]K_i values are presented as "mean [95% confidence interval]" and were determined using ^{nat}Ga compound and [^{125}I]I-Tyr^3-neurotensin as the radioligand. [b]Percentage of intact compound after 4 h incubation in mouse serum at 37 °C using ^{nat}Ga compounds. [c]Partition coefficients (log*D*) were determined at pH 7.4 using ^{68}Ga compounds and are presented as mean. N.D.: not determined.

good stability of small molecules relative to peptides. For comparison, only 55% of the natural neurotensin was found intact after 4 h of incubation in the same assay conditions (Table S1).

***In Vitro* Binding Affinity.** The affinity for NTS_1 of the seven ^{nat}Ga-metalated compounds and the reference ^{nat}Ga-3BP-227 was determined in a competition experiment on CHO cells overexpressing the NTS_1 receptor. [^{125}I]I-Tyr^3-neurotensin (0.05 nM; K_d = 0.22 nM) was used as a ligand.[49] The K_i values were in the nanomolar range for most of the compounds (Table 1 and Figure S48). The compounds with a single chelator showed the best affinities with K_i values between 0.7 and 3.6 nM, similar to the reference ^{nat}Ga-3BP-227 (0.55 nM). According to these results, it seems that the presence of a positive charge favors binding to NTS_1 (^{nat}Ga-NOTA-**16**, K_i 0.73 nM), and conversely, an increase in the number of negative charges has a detrimental effect on affinity (^{nat}Ga-DOTAGA-**16**, K_i 3.59 nM). In comparison, the compounds with two chelating agents showed a significant decrease in affinity (K_i of 9 nM and 62 nM for ^{nat}Ga-bisNODAGA-**16** and ^{nat}Ga-bisDOTAGA-**16**, respectively).

Radiolabeling and Partition Coefficients. All the compounds were radiolabeled with ^{68}Ga, using [^{68}Ga]$GaCl_3$ obtained after elution of a generator with a 0.1 M HCl solution. A solution of sodium acetate buffer (0.5 M, pH 5.56) was added to the compounds in order to reach a final pH of 3.5. Ten percent of ethanol was also introduced to limit radiolysis. The radiolabeling of NOTA, NODAGA, and THP-based compounds was performed at 37 °C for 5 min, whereas 10 min at 95 °C were required to radiolabel DOTA and DOTAGA-based compounds. Each tracer was purified on a C_{18} Sep-Pack column to obtain the desired compound with a radiochemical purity of >94%, as determined by radio-HPLC. The radiochemical yields ranged from 35% to 80% and molar activities from 8.8 to 17.8 MBq/nmol at the end of radiolabeling. Partition coefficients (log*D*) were determined by the shake-flask method in octanol and PBS at pH 7.4.[50] All compounds were found to be hydrophilic. As expected, compounds with two chelating agents are more hydrophilic with log*D* values of about −3.5 while values ranging from −1.7 to −2.6 are obtained for compounds with only one chelating agent. The compound [^{68}Ga]Ga-THP-**16** is the least hydrophilic of all with a log*D* of −1.2 (Table 1).

Table 2. *Ex Vivo* Biodistribution and Tumor-to-Organ Ratios of 3BP-227, 3BP-228, and DOTA-NT-20.3[a]

	[^{68}Ga]Ga-3BP-228	[^{68}Ga]Ga-3BP-227	[^{68}Ga]Ga-DOTA-NT-20.3
uptake (%ID/g)	*n* = 4	*n* = 4	*n* = 4
blood	1.083 ± 0.222	9.155 ± 0.705***	0.088 ± 0.017*
liver	0.908 ± 0.129	3.725 ± 2.181*	0.103 ± 0.022
gallbladder	3.347 ± 3.208	4.240 ± 1.786	0.108 ± 0.071
kidneys	2.525 ± 0.641	4.775 ± 1.055*	5.705 ± 1.457**
spleen	0.408 ± 0.085	1.610 ± 0.147***	0.113 ± 0.026**
heart	0.555 ± 0.102	3.518 ± 0.843***	0.053 ± 0.019
lungs	1.060 ± 0.164	4.675 ± 0.429***	0.173 ± 0.036**
muscle	0.348 ± 0.345	0.985 ± 0.114**	0.025 ± 0.010
intestine	1.093 ± 0.098	2.018 ± 0.497**	0.405 ± 0.072*
carcass	1.125 ± 0.560	4.253 ± 0.621***	0.160 ± 0.022*
tumor	7.825 ± 2.507	11.238 ± 1.704*	1.655 ± 0.497**
tumor-to-organ ratios	*n* = 4	*n* = 4	*n* = 4
blood	7.540 ± 2.938	1.243 ± 0.279	19.08 ± 5.778**
intestine	1.093 ± 0.098	2.018 ± 0.497**	0.405 ± 0.072*
kidneys	3.125 ± 0.695	2.393 ± 0.346	0.300 ± 0.110**

[a]Top: *Ex vivo* biodistribution of [^{68}Ga]Ga-3BP-228, [^{68}Ga]Ga-3BP-227, and [^{68}Ga]Ga-DOTA-NT-20.3, 2 h p.i. Values are expressed as the percentage of injected dose per gram of tissue (%ID/g ± SD). Bottom: Tumor-to-organ ratios from the *ex vivo* biodistribution. Values are expressed as means ± SD. Statistical analysis by one-way ANOVA with [^{68}Ga]Ga-3BP-228 as a control group, followed by Bonferroni correction, *p < 0.05, **p < 0.01, and ***p < 0.001.

https://doi.org/10.1021/acs.jmedchem.1c00523
J. Med. Chem. 2021, 64, 8564−8578

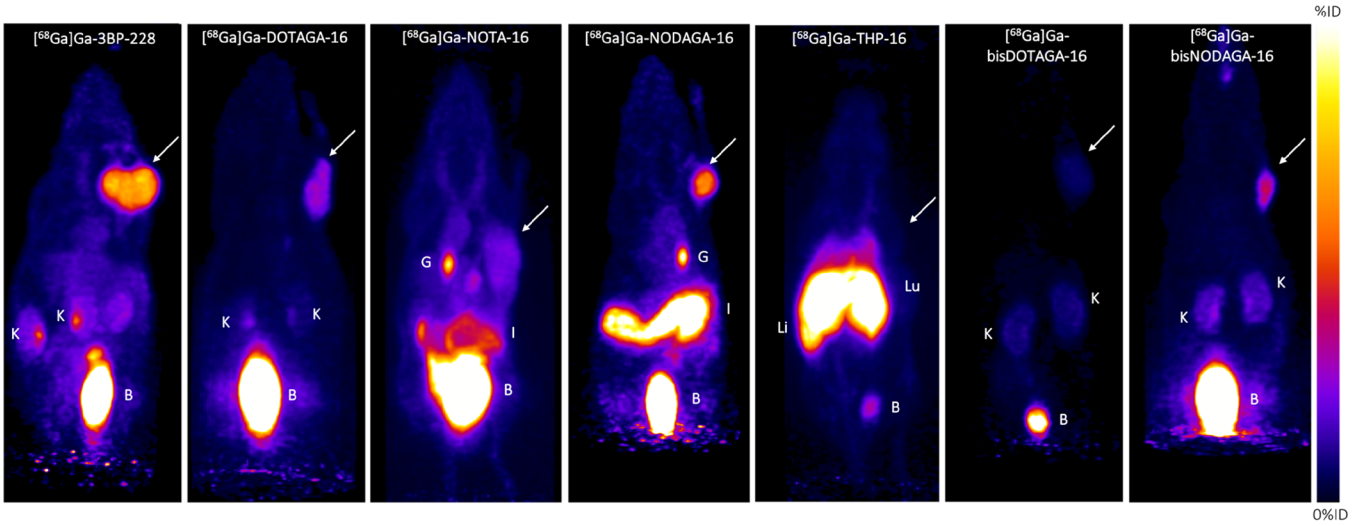

Figure 2. Maximum intensity projection (MIP) images obtained between 1.5 h and 2 h p.i. of [^{68}Ga]Ga-3BP-228, [^{68}Ga]Ga-DOTAGA-**16**, [^{68}Ga]Ga-NOTA-**16**, [^{68}Ga]Ga-NODAGA-**16**, [^{68}Ga]Ga-THP-**16**, [^{68}Ga]Ga-bisDOTAGA-**16**, and [^{68}Ga]Ga-bisNODAGA-**16**. The tumor is showed by a white arrow. Abbreviations: G, gallbladder; I, intestines; K, kidneys; B, bladder; Li, liver; Lu, lungs.

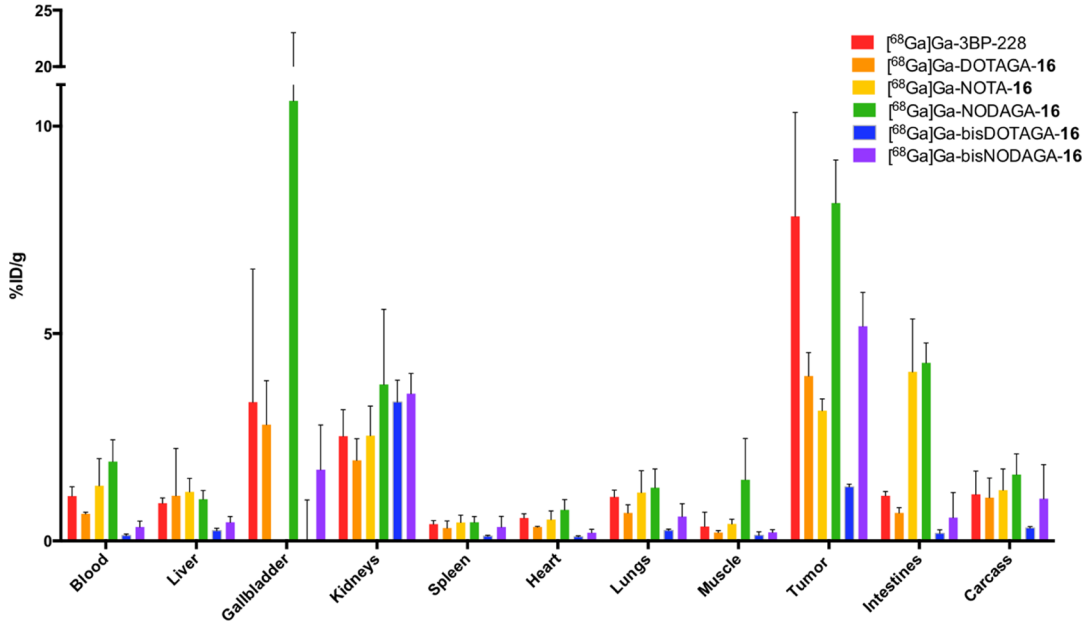

Figure 3. *Ex vivo* biodistribution data of ^{68}Ga compounds 2 h p.i. Values are expressed as the percentage of injected dose per gram (%ID/g, mean ± SD) for each collected organ. Data for [^{68}Ga]Ga-THP-**16** are presented in Table S2.

PET-MRI Imaging and Biodistribution. In order to evaluate the biodistribution of each compound, the radiolabeled tracers were injected intravenously (500 pmol, 3−8 MBq) in the lateral tail vein of nude mice bearing a xenograft of human colorectal cancer (HT-29) in the flank. This tumor model expresses NTS_1.[49] Static PET-MRI images were recorded between 1.5 h and 2 h post-injection.

First, we chose to compare [^{68}Ga]Ga-3BP-228 to two references: [^{68}Ga]Ga-3BP-227 and a well-validated NTS_1 peptide agonist named [^{68}Ga]Ga-DOTA-NT-20.3.[51,52,11] As could be expected from the results of Schulz *et al.* with ^{111}In-labeled compounds, [^{68}Ga]Ga-3BP-228 showed faster blood clearance than its isomer. Indeed, a high level of circulating activity was observed for [^{68}Ga]Ga-3BP-227, leading to a tumor-to-blood ratio of 1.243 ± 0.279 while a ratio of 7.540 ± 2.938 was obtained with [^{68}Ga]Ga-3BP-228 (Table 2 and Figure S49).

In comparison, [^{68}Ga]Ga-DOTA-NT-20.3 showed a typical biodistribution profile for a NTS_1 peptide agonist, with a lower uptake in the tumor compared to [^{68}Ga]Ga-3BP-228, but a minimal activity in all the other tissues (apart from kidneys), giving tumor-to-organ ratios around two times higher than [^{68}Ga]Ga-3BP-228 for the blood, liver, muscle, and heart (Table 2 and Figure S49).

Overall, these results showed that NTS_1 small molecule antagonists have a good potential for ^{68}Ga-PET diagnosis but that their pharmacokinetics needed to be further optimized.

Next, we undertook the evaluation of our seven novel derivatives. All these compounds showed important differences in terms of biodistribution. For instance, administration of the THP derivative gave a much stronger signal in the lungs, spleen, and liver (12.7 ± 4.1%ID/g, 46.4 ± 9.3%ID/g, and 42.0 ± 8.1% ID/g, respectively) than all the other compounds (0.5−1.3%ID/

https://doi.org/10.1021/acs.jmedchem.1c00523
J. Med. Chem. 2021, 64, 8564−8578

Table 3. *Ex Vivo* Biodistribution and Tumor-to-Organ Ratios at 2 h p.i.[a]

uptake (%ID/g)	[68Ga]Ga-3BP-228 $n = 4$	[68Ga]Ga-DOTAGA-**16** $n = 4$	[68Ga]Ga-NOTA-**16** $n = 4$	[68Ga]Ga-NODAGA-**16** $n = 4$	[68Ga]Ga-bisDOTAGA-**16** $n = 4$	[68Ga]Ga-bisNODAGA-**16** $n = 4$	[68Ga]Ga-DOTA-NT-20.3 $n = 4$
blood	1.083 ± 0.222	0.658 ± 0.039	1.330 ± 0.654	1.915 ± 0.526	0.135 ± 0.031*	0.393 ± 0.108	0.088 ± 0.017*
liver	0.908 ± 0.129	0.523 ± 0.025	1.183 ± 0.325	1.005 ± 0.211	0.250 ± 0.057	0.387 ± 0.072	0.103 ± 0.022
gallbladder	3.347 ± 3.208	2.803 ± 1.062	-	10.610 ± 12.404	0.367 ± 0.040	1.363 ± 0.993	0.108 ± 0.071
kidneys	2.525 ± 0.641	1.943 ± 0.525	2.540 ± 0.713	3.775 ± 1.811	3.353 ± 0,523	3.377 ± 0.425	5.705 ± 1.457**
spleen	0.408 ± 0.085	0.310 ± 0.174	0.445 ± 0.177	0.448 ± 0.141	0.118 ± 0.019	0.207 ± 0.025	0.113 ± 0.026**
heart	0.555 ± 0.102	0.335 ± 0.019	0.518 ± 0.205	0.750 ± 0.249	0.103 ± 0.021**	0.167 ± 0.038*	0.053 ± 0.019
lungs	1.060 ± 0.164	0.678 ± 0.194	1.165 ± 0.527	1.285 ± 0.452	0.255 ± 0.031	0.437 ± 0.071	0.173 ± 0.036**
muscle	0.348 ± 0.345	0.205 ± 0.044	0.413 ± 0.114	1.475 ± 0.997**	0.138 ± 0.083	0.210 ± 0.061	0.025 ± 0.010
intestine	1.093 ± 0.098	0.678 ± 0.127	4.080 ± 1.272	4.293 ± 0.483	0.183 ± 0.083	0.267 ± 0.097	0.405 ± 0.072*
carcass	1.125 ± 0.560	1.043 ± 0.474	1.225 ± 0.513	1.603 ± 0.496	0.313 ± 0.036	0.610 ± 0.154	0.160 ± 0.022*
tumor	7.825 ± 2.507	3.978 ± 0.564***	3.140 ± 0.286***	8.148 ± 1.038	1.305 ± 0.062***	4.917 ± 0.776*	1.655 ± 0.497**
tumor-to-organ ratios	$n = 4$	$n = 4$	$n = 4$	$n = 4$	$n = 4$	$n = 4$	$n = 4$
blood	7.540 ± 2.938	6.093 ± 1.173	2.788 ± 1.172*	4.468 ± 1.085	10.028 ± 2.189	13.190 ± 4.216*	19.083 ± 5.778**
intestine	7.145 ± 2.064	6.125 ± 2.026	0.808 ± 0.167*	1.900 ± 0.177	8.843 ± 5.184	19.747 ± 5.633***	4.290 ± 1.899
kidneys	3.125 ± 0.695	2.158 ± 0.655	1.288 ± 0.244**	2.555 ± 1.116	0.393 ± 0.051	1.450 ± 0.053**	0.300 ± 0.110***

[a]Values are expressed as mean ± SD. Data for THP-**16** are shown in Tables S2 and S3. Statistical analysis by one-way ANOVA with [68Ga]Ga-3BP-228 as a control group, followed by Bonferroni correction, *$p < 0.05$, **$p < 0.01$, and ***$p < 0.001$.

g) (Figure 2). Moreover, the tumor uptake of [68Ga]Ga-THP-**16** was very low (1.33 ± 0.35%ID/g) (Tables S2 and S3 and Figure S49). We assume that this behavior results from the lipophilicity of the THP moiety.[S3] Indeed, [68Ga]Ga-THP-**16** has a log*D* of −1.17 while the other compounds have logD values between −1.75 and −3.62 (Table 1).

The other four compounds, labeled with a single macrocyclic chelator, gave fairly similar profiles for most organs. The main difference was observed in the gallbladder and intestines (Figures 2 and 3). Indeed, the NOTA/NODAGA compounds showed a much stronger signal in these organs than DOTA/DOTAGA compounds, suggesting a partial hepatobiliary excretion pathway for these derivatives. This may limit their interest for the imaging of abdominal tumors. Concerning tumor uptake, we observed on PET images that the compounds [68Ga]Ga-NODAGA-**16** and [68Ga]Ga-3BP-228 showed a better accumulation in the tumor than [68Ga]Ga-NOTA-**16** and [68Ga]Ga-DOTAGA-**16** (Figure 2). Indeed, for the NODAGA- and DOTA-based compound, a signal of about 8%ID/g 2 h p.i. was observed while the NOTA- and DOTAGA-based compounds gave only 3−4%ID/g (Figure 3). However, the best tumor-to-organ ratios were observed for the tracers [68Ga]Ga-3BP-228 and [68Ga]Ga-DOTAGA-**16** (Table 3).

Next, the introduction of two chelating agents on the same molecule was attempted with the objective to speed up the clearance of the tracer from non-targeted tissues. The corresponding PET images showed high contrast, with less than 0.4%ID/g in blood after 2 h (Figure 2). The bisDOTAGA derivative, [68Ga]Ga-bisDOTAGA-**16**, showed very little signal in all organs but also a rather low tumor uptake (1.305 ± 0.062% ID/g), leading to tumor-to-organ ratios quite similar to those obtained with the corresponding single-chelator [68Ga]Ga-DOTAGA-**16** (Figure 3 and Table 3). We assume that the limited retention in the tumor tissue is probably related to its reduced affinity for NTS_1 (K_i = 61.9 nM) compared to the other molecules. In contrast, [68Ga]Ga-bisNODAGA-**16** showed an attractive biodistribution profile with less signal in all non-targeted organs while retaining a good tumor uptake value of 4.917 ± 0.776%ID/g, leading to the best tumor-to-organ ratios (Figures 2 and 3 and Table 3). Interestingly, this compound did not accumulate in the gallbladder and intestines.

In order to evaluate the specificity for NTS_1, a blocking experiment (in the presence of a 100-fold molar excess of SR142948A) was carried out with the tracers [68Ga]Ga-bisNODAGA-**16**, [68Ga]Ga-DOTAGA-**16**, and [68Ga]Ga-3BP-228. The uptake in all isolated organs remained essentially unchanged, apart from tumor uptake whose value decreased by a factor of 2 to 5 (Figure 4 and Table S4). PET-MRI imaging confirmed the biodistribution results (Figure S50). These results demonstrate the specificity of these tracers for neurotensin receptor-positive tumors.

***In Vitro* and *In Vivo* Evaluation of [68Ga]Ga-bisNODAGA-16.** In order to determine whether the uptake of the tracer bisNODAGA-**16** in HT29 tumor was mediated by NTS_1, NTS_2,

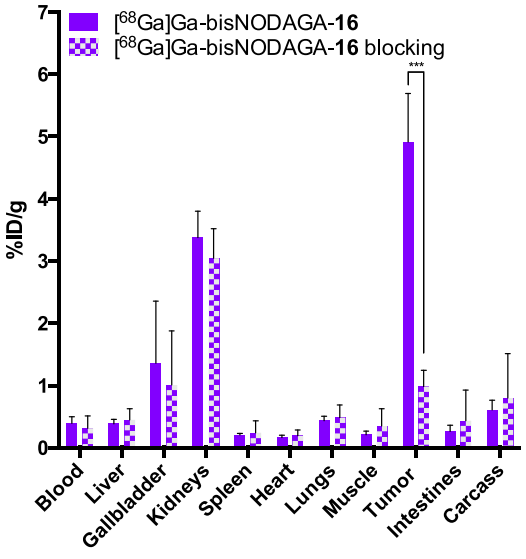

Figure 4. *Ex vivo* biodistribution of [68Ga]Ga-bisNODAGA-**16** 2 h p.i., with or without a 100-fold excess of SR142948A. Data were analyzed by an unpaired two-tailed Student's *t*-test (***$p < 0.001$).

https://doi.org/10.1021/acs.jmedchem.1c00523
J. Med. Chem. 2021, 64, 8564−8578

or both receptors, an *in vitro* competition assay on HT29 cells was performed (Figure S51). The binding of [^{68}Ga]Ga-bisNODAGA-**16** to HT29 cells was inhibited by an excess of SR142948A or neurotensin, but not by levocabastine, a histamine H_1 receptor antagonist that blocks NTS_2.[20] These results suggest that the tumor uptake observed *in vivo*, in this model, is primarily due to binding to NTS_1. The antagonistic properties of the lead compound ^{nat}Ga-bisNODAGA-**16** were confirmed in a calcium flux mobilization assay performed on CHO cells expressing human recombinant NTS_1 (IC_{50} = 141 nM; K_B = 13 nM; Figure S52).

[^{68}Ga]Ga-bisNODAGA-**16** was further evaluated in a model of pancreatic ductal adenocarcinoma (subcutaneous xenografts of human AsPC-1 tumor cells).[11] PET/CT images were recorded 50−70 min and 90−110 min after injection (Figure S53). Tumor masses could be easily detected as early as 60 min after injection. A post-mortem biodistribution study was performed 2 h post-injection, which confirmed the accumulation of the radioactive tracer in the tumor (Table S5).

CONCLUSIONS

Since the discovery of NTS_1 receptor overexpression in many tumors, considerable efforts have been undertaken to develop NTS_1-targeted radiopharmaceuticals that may improve cancer diagnosis and stratification (the reader is encouraged to refer to Maschauer and Prante's excellent review on the topic).[12] Unfortunately, despite extensive optimization work, a very few tracers based on neurotensin peptide analogs have been tested in patients, and their results have so far been disappointing.[16,54,55] In this context, the emergence of nonpeptide antagonist radioligands of NTS_1 is a new source of hope. While efforts have until now been concentrated on ^{177}Lu-labeling of these compounds for internal vectorized radiotherapy, here we investigated whether they could be adapted to the elaboration of NTS_1-specific ^{68}Ga-PET imaging tracers to form a theranostic pair.

In a seminal paper published in 2012, Fani *et al.* stated that "the chelate makes the difference", stressing that the structure of a chelating agent can greatly influence the biodistribution of a tracer.[56] Since then, numerous teams confirmed this observation.[35−38,40,57−61] By evaluating seven different chelating agents introduced on the same NTS_1 antagonist molecule, we were able to identify a promising new PET tracer, [^{68}Ga]Ga-bisNODAGA-**16**, that showed rapid accumulation in the tumor (4.917 ± 0.776%ID/g, 2 h p.i.) and fast clearance from blood and other organs. This behavior led to contrasted PET-MRI images, with tumor-to-organ ratios of 1.45 ± 0.05, 13.2 ± 4.2, to 24.9 ± 8.6 for the kidneys, blood, and muscle, respectively. This antagonist showed a biodistribution profile similar to that of the agonist peptide analogue [^{68}Ga]Ga-DOTA-NT-20.3, with comparable or even better tumor-to-organ ratios for organs such as kidneys, spleen, heart, lungs, and intestines.

Unfortunately, to date, the effect of the chelating agent on the pharmacokinetics of a tracer is still hard to predict and needs to be evaluated *in vivo*. For example, although a study by Young's *et al.* has found that the introduction of THP on a PSMA radiotracer could give very good results,[62] in our study, the THP derivative showed poor tumor uptake and high accumulation in the spleen, kidneys, and lungs. While tracers such as [^{68}Ga]Ga-JMV6659 show NTS_1-mediated accumulation in the spleen and blood (which the authors suggest is related to specific binding to NTS_1 expressed on blood cells),[63] we believe that the observed biodistribution for [^{68}Ga]Ga-THP-**16** results primarily from its lipophilicity (or lack of *in vivo* stability), which leads to unfavorable hepatobiliary clearance. Several studies have suggested that the charge of the chelate would have a major impact on the biodistribution.[39,58,36] In our specific case, compounds with neutral charge complexes presented a better tumor accumulation *in vivo*.

On a positive note, it appears that the addition of an extra-chelator is a reliable and straightforward strategy to speed up the renal excretion of tracers, leading to better images, provided that the affinity is retained.[41] In addition, it increases the molar activities that can be potentially achieved. However, it should be noted that this approach may complicate the pharmaceutical development of the tracer as it is difficult to predict which chelator binds to the radiometal. Saturation of the molecule with ^{nat}Ga, after radiolabeling, may be necessary to obtain a homogeneous tracer.

EXPERIMENTAL SECTION

General Information. All chemicals were purchased from Merck, Acros Organics, and Alfa Aesar and used without further purification. DOTA-NHS, DOTAGA-anhydride, NOTA-NHS, (*R*)-NODAGA-NHS, THP-NCS, DOTAGA(tBu)$_4$, and NODAGA(tBu)$_3$ were provided by CheMatech (Dijon, France). Moisture-sensitive reactions were performed under a nitrogen or argon atmosphere. The purity of final compounds was determined by RP-HPLC-MS and was >95% for all tested compounds unless stated.

Experimental Procedures and Characterization Data for Synthon A. *2-Isopropylacetanilide (**1**).* A solution containing 2-isopropylaniline (5 mL, 35.3 mmol, 1 equiv) and toluene (48 mL) was cooled in an ice bath. Acetic anhydride (3.52 mL, 37.1 mmol, 1.05 equiv) was added slowly. After stirring for 45 min at RT, the reaction medium was evaporated. The red oil obtained was then taken up with petroleum ether (15 mL). The white precipitate formed was filtered and dried under vacuum to give a white solid (5.83 g, 93%, purity >99%). RP-HPLC-MS: t_r = 3.82 min, m/z calculated for $C_{11}H_{15}NO$ $[M + H]^+$ 178.1, found 178.0. R_f (CH_2Cl_2/MeOH, 98/2) = 0.26. ^{1}H-NMR (500 MHz, $CDCl_3$): δ = 1.25 (d, J = 6.8 Hz, 6H), 2.2 (s, 3H), 3.05 (hept, J = 6.8 Hz, 1H), 7−7.3 (m, 4H), 7.6 (m, 1H) ppm; ^{13}C-NMR (126 MHz, $CDCl_3$): δ = 23.2 (CH_3), 24.3 (CH_3), 28.1 (CH), 125.4 (CH), 125.8 (CH), 126.4 (CH), 126.5 (CH), 134.1 (C), 141.1 (C), 168.9 (C) ppm. mp: 72 °C.

*4-Bromo-2-isopropylacetanilide (**2**).* A solution of *N*-bromosuccinimide (7.53 g, 42.3 mmol, 1.5 equiv) in DMF (14 mL) was added dropwise over 45 min to a solution of 2-isopropylacetanilide (**1**) (5 g, 28.2 mmol, 1 equiv) in DMF (14 mL). The mixture was stirred at RT overnight. The reaction mixture was evaporated to obtain a yellow oil, extracted with CH_2Cl_2, washed with acidic water and brine, and dried over $MgSO_4$. The solvent was evaporated to give a yellow solid, which was purified by flash-column chromatography (A: CH_2Cl_2, B: CH_2Cl_2/MeOH 9:1; with the following gradient program: 0% to 40% of B in 25 CV). A white solid (4.62 g, 64%, purity: 93%) was obtained. RP-HPLC-MS: t_r = 4.26 min, m/z calculated for $C_{11}H_{14}BrNO$ $[M - H]^-$ 254.0, found 254.0. R_f (CH_2Cl_2/MeOH, 98/2) = 0.32. ^{1}H-NMR (500 MHz, $CDCl_3$): δ = 1.23 (d, J = 6.8 Hz, 6H), 2.19 (s, 3H), 2.98 (hept, J = 6.8 Hz, 1H), 7.00 (br, 1H), 7.30 (d, J = 8.5 Hz, 1H), 7.38 (s, 1H), 7.53 (d, J = 8.5 Hz,1H) ppm; ^{13}C-NMR (126 MHz, $CDCl_3$): δ = 23.0 (CH_3), 24.3 (CH_3), 28.2 (CH), 119.7 (C), 126.8 (CH), 129.0 (CH), 129.6 (CH), 133.2 (C), 143.0 (C), 168.8 (C) ppm. mp: 132 °C.

*4-Cyano-2-isopropylacetanilide (**3**).* A mixture of 4-bromo-2-isopropylacetanilide (**2**) (4.8 g, 18.74 mmol, 1 equiv), DMF (22.5 mL), cuprous cyanide (2.51 g, 28.1 mmol, 1.5 equiv), and water (0.370 mL) was stirred under reflux overnight. After cooling, the reaction medium was concentrated under vacuum and water (58 mL) was added to the mixture under stirring. The precipitate was filtered off, rinsed with water, and dried under vacuum. The gray/brown solid was purified by flash-column chromatography (A: CH_2Cl_2, B: CH_2Cl_2/MeOH 9:1; with the following gradient program: 0% to 40% of B in 25 CV). A white solid (1.23 g, 33%, purity: 95%) was obtained. RP-HPLC-MS: t_r = 3.65

https://doi.org/10.1021/acs.jmedchem.1c00523
J. Med. Chem. 2021, 64, 8564−8578

min, m/z calculated for $C_{12}H_{14}N_2O$ $[M - H]^-$ 201.1, found 201.1. ^{1}H-NMR (500 MHz, $CDCl_3$): δ = 1.28 (d, J = 6.8 Hz, 6H), 2.24 (s, 3H), 3.01 (hept, J = 6.8 Hz, 1H), 7.25 (br, 1H), 7.49 (d, J = 8.5 Hz, 1H), 7.54 (s, 1H), 8.08 (d, J = 8.5 Hz, 1H) ppm; ^{13}C-NMR (126 MHz, $CDCl_3$): δ = 22.6 (CH_3), 24.7 (CH_3), 27.8 (CH), 108.4 (C), 119.1 (C), 123.4 (CH), 129.8 (CH), 130.5 (CH), 138.5 (C), 168.4 (C) ppm. mp: 139 °C.

*4-Cyano-2-isopropylaniline Hydrochloride (**4**).* A mixture of 4-cyano-2-isopropylacetanilide (**3**) (2.5 g, 15.3 mmol, 1 equiv), absolute ethanol (12 mL), and 1 N HCl (12 mL) was stirred under reflux for 3 days. A solution of 10% NaOH (7 mL) was added to reach a pH of 10. The reaction medium was extracted three times with CH_2Cl_2, and the organic layers were combined, dried over $MgSO_4$, and concentrated under vacuum. The orange oil obtained was dissolved in diethyl ether (36 mL), and 1 M ethereal hydrogen chloride (10 mL) was added. The white precipitate was filtered off and rinsed with diethyl ether to give the expected product (2.21 g, 74%, purity: 91%). RP-HPLC-MS: t_r = 4.22 min, m/z calculated for $C_{10}H_{13}N_2^+$ $[M + CH_3CN]^+$ 202.3, found 202.1. ^{1}H-NMR (500 MHz, DMSO-d_6): δ = 1.14 (d, J = 6.8 Hz, 6H), 2.96 (hept, J = 6.8 Hz, 1H), 6.72 (d, J = 8.3 Hz, 1H), 7.28 (d, J = 8.3 Hz, 1H), 7.34 (s, 1H) ppm; ^{13}C-NMR (126 MHz, DMSO-d_6): δ = 22.4 (CH_3), 26.7 (C), 107.4 (C), 115.1 (C), 121.3 (CH), 129.7 (CH), 131.1 (CH) ppm. mp: 186 °C.

*4-Amino-3-isopropylbenzoic Acid Hydrochloride (**5**).* A solution of potassium hydroxide (16.8 g, 0.3 mol, 20 equiv), water (18 mL), and 1,2-dimethoxyethane (1.5 mL) was added to 4-cyano-2-isopropylaniline hydrochloride (**4**) (3.0 g, 15.0 mmol, 1 equiv). The mixture was heated to reflux for 3 days. After cooling, concentrated HCl (12 mL) was added to reach a pH of 1 and the mixture was then extracted three times with CH_2Cl_2. The organic layers were combined, dried over $MgSO_4$ and concentrated to yield an orange solid (2.42 g, 75%, purity: 97%). RP-HPLC-MS: t_r = 3.33 min, m/z calculated for $C_{10}H_{13}NO_2$ $[M + H + CH_3CN]^+$ 221.1, found 221.0. R_f (CH_2Cl_2/MeOH, 98/2) = 0.3. ^{1}H-NMR (500 MHz, $CDCl_3$): δ = 1.30 (d, J = 6.8 Hz, 6H), 2.85 (hept, J = 6.8 Hz, 1H), 6.66 (d, J = 8.3 Hz, 1H), 7.80 (dd, J = 8.3, 1.9 Hz, 1H), 7.92 (d, J = 1.9 Hz, 1H) ppm; ^{13}C-NMR (126 MHz, $CDCl_3$): δ = 22.1 (CH_3), 27.8 (CH), 114.7 (CH), 119.1(C), 128.5 (CH), 129.8 (CH), 131.4 (C), 148.9 (C), 172.5 (C) ppm. mp: 130 °C.

*3-Isopropyl-4-hydrazinobenzoic Acid Hydrochloride (Synthon **A**).* A solution of concentrated HCl (25 mL) and AcOH (22 mL) was added to 4-amino-3-isopropylbenzoic acid hydrochloride (**5**) (1.3 g, 6.0 mmol, 1 equiv). The mixture was cooled to −5 °C, and a solution of $NaNO_2$ (0.62 g, 9.0 mmol, 1.5 equiv) in water (4.5 mL) was added dropwise over 10 min. The mixture was stirred at 0 °C for 3 h and then cooled to −10 °C. A solution of stannous chloride dihydrate (4.11 g, 18.0 mmol, 3.1 equiv) in concentrated HCl (4.5 mL) was added slowly. The temperature was allowed to rise to RT, and the precipitate formed was filtered off after 2 h and rinsed with 1 M HCl (5 mL). A yellowish powder (1.29 g, 93%, purity: 89%) was obtained after drying over P_2O_5. RP-HPLC-MS: t_r = 0.4 min, m/z calculated $C_{10}H_{14}N_2O_2$ $[2 M + H]^+$ 389.2, found 389.2. ^{1}H-NMR (500 MHz, DMSO-d_6): δ = 1.19 (d, J = 6.8 Hz, 6H), 3.14 (hept, J = 6.8 Hz, 1H), 6.98 (d, J = 8.4 Hz, 1H), 7.76 (d, J = 8.4 Hz, 1H), 7.78 (s, 1H), 8.31 (br, 1H) ppm; ^{13}C-NMR (126 MHz, DMSO-d_6): δ = 22.9 (CH_3), 26.5 (CH), 112.6 (CH), 124.0 (C), 127.0 (CH), 128.5 (CH), 134.7 (C), 146.1 (C), 167.6 (C) ppm. mp: 245 °C.

Experimental Procedures and Characterization Data for Synthon B. *Ethyl-4-(2,6-Dimethoxyphenyl)-4-hydroxy-2-oxobut-3-enoate (Synthon **B**).* Sodium hydride 60% (0.40 g, 9.96 mmol, 1.2 equiv) was added to a solution of diethyl oxalate (1.36 g, 9.96 mmol, 1.2 equiv) in DMF (5 mL), and the mixture was stirred for 5 min. A solution of 2,6-dimethoxyacetophenone (1.5 g, 8.3 mmol, 1 equiv) in DMF (5 mL) was slowly added over 15 min. The mixture was then stirred at RT overnight. The reaction medium was extracted with EtOAc three times, ensuring that the pH remained below 6 between each extraction. The organic layers were combined, dried over $MgSO_4$, and concentrated under vacuum. Following recrystallization from EtOH, a yellowish powder (1.7 g, 73%, purity: 90%) was obtained. RP-HPLC-MS: t_r = 4.90 min, m/z calculated for $C_{14}H_{16}O_6$ $[M + H]^+$ 281.1, found 281.1. ^{1}H-NMR (500 MHz, $CDCl_3$): δ = 1.37 (t, J = 7.1 Hz, 3H), 3.82 (s, 6H), 4.35 (q, J = 7.1 Hz, 2H), 6.59 (d, J = 8.4 Hz, 2H), 6.61 (s, 1H), 7.34 (t, J = 8.4 Hz, 1H), 14.33 (br 1H) ppm; ^{13}C-NMR (126 MHz, $CDCl_3$): δ = 14.2 (CH_3), 56.2 (CH_3), 62.5 (CH_2), 104.2 (CH), 106.4 (CH), 117.2 (C), 132.4 (CH), 158.0 (C), 162.6 (C), 163.9 (C), 195.9 (C) ppm. mp: 103 °C.

Experimental Procedures and Characterization Data for 6. *4-(5-(2,6-Dimethoxyphenyl)-3-(ethoxycarbonyl)-1H-pyrazol-1-yl)-3-isopropylbenzoic Acid (**6**).* A mixture of 3-isopropyl-4-hydrazinobenzoic acid hydrochloride (synthon **A**) (0.56 g, 2.4 mmol, 1.05 equiv) and ethyl-4-(2,6-dimethoxyphenyl)-4-hydroxy-2-oxobut-3-enoate (synthon **B**) (0.65 g, 2.3 mmol, 1 equiv) in AcOH (8.5 mL) was stirred under reflux for 4 days. The brownish suspension was poured into 15 mL of ice-water bath, and the yellow precipitate was filtered off and washed with water. The yellow solid was purified on a silica plug (CH_2Cl_2 to CH_2Cl_2/MeOH 9:1) to obtain the expected product (0.8 g, 80%, purity: 92%). RP-HPLC-MS: t_r = 5.1 min, m/z calculated for $C_{24}H_{26}N_2O_6$ $[M + H]^+$ 439.2, found 439.2. R_f (CH_2Cl_2/MeOH, 9/1) = 0.52. ^{1}H-NMR (500 MHz, DMSO-d_6): δ = 0.96 (d, J = 5.3 Hz, 6H), 1.31 (t, J = 7.1 Hz, 3H), 2.65 (m, 1H), 3.61 (s, 6H), 4.31 (q, J = 7.1 Hz, 2H), 6.60 (d, J = 8.5 Hz, 2H), 6.83 (s, 1H), 7.28 (d, J = 8.2 Hz, 1H), 7.31 (t, J = 8.5 Hz, 1H), 7.76 (dd, J = 8.2, 1.8 Hz, 1H), 7.85 (d, J = 1.8 Hz, 1H), 13.19 (br, 1H) ppm; ^{13}C-NMR (126 MHz, DMSO-d_6): δ = 14.7 (CH_3), 27.6 (CH_3), 40.6 (CH), 56.0 (CH_3), 60.8 (CH_2), 104.3 (CH), 106.1 (C), 111.2 (CH), 127.0 (CH), 127.4 (CH), 128.6 (CH), 132.20 (C), 132.2 (CH), 139.2 (C), 141.2 (C), 143.7 (C), 146.0 (C), 158.4 (C), 162.2 (C), 167.1 (C) ppm.

Experimental Procedures and Characterization Data for 3BP-227. *Benzyl Methyl(3-(methyl(3-(methylamino)propyl)-amino)propyl)carbamate (synthon **E**).* A solution of *N,N*-bis[3-(methylamino)propyl]methylamine (2 mL, 11 mmol, 5 equiv) in CH_2Cl_2 (15 mL) was cooled to −78 °C. To this solution was added dropwise a solution of benzyl chloroformate (0.3 mL, 2.2 mmol, 1 equiv) in CH_2Cl_2 (6 mL) over 1 h. The reaction was stirred at −78 °C for 1.5 h before warming to room temperature and stirred for another 15 h. The white suspension obtained was washed twice with a solution of K_2CO_3 5%, twice with brine, dried over $MgSO_4$, filtered, and concentrated under vacuum. The colorless oil obtained was purified by semi-preparative RP-HPLC. A colorless oil (0.542 g, 80%, purity: 94%) was isolated. RP-HPLC-MS: t_r = 0.32 min, m/z calculated for $C_{17}H_{29}N_3O_2$ $[M + H]^+$ 308.2, found 308.2. ^{1}H-NMR (500 MHz, $CDCl_3$): δ = 1.95 (m, 2H), 2.21 (m, 2H), 2.66 (s, 3H), 2.76 (m, 4H), 2.91 (s, 3H), 3.07 (m, 5H), 3.34 (m, 2H), 5.09 (s, 2H), 5.76 (br, NH_2^+), 7.3−7.4 (m, 5H), 9.30 (br, NH^+) ppm. ^{13}C-NMR (126 MHz, $CDCl_3$): δ = 21.1 (CH_2), 22.4 (CH_2), 33.3 (CH_3), 39.8 (CH_3), 45.9 (CH_3), 46.2 (CH_2), 53.1 (CH_2), 54.3 (CH_2), 67.6 (CH_2), 116.0 (q, TFA), 127.6 (CH), 128.2 (CH), 128.6 (CH), 136.4 (C), 157.2 (C), 161.3 (q, TFA) ppm.

*Ethyl 1-(4-((3-((3-((((Benzyloxy)carbonyl)(methyl)amino)propyl)-(methyl)amino)propyl)(methyl)carbamoyl)-2-isopropylphenyl)-5-(2,6-dimethoxyphenyl)-1H-pyrazole-3-carboxylate (**7**).* To a solution of **6** (200 mg, 0.46 mmol, 1 equiv) in anhydrous DMF (2 mL) was added DIPEA (96 μL, 0.55 mmol, 1.2 equiv) and HATU (228 mg, 0.6 mmol, 1.3 equiv). The solution was stirred 20 min at RT. A solution of benzyl methyl(3-(methyl(3-(methylamino)propyl)amino)propyl)-carbamate (TFA salt) (synthon **E**) (169 mg, 0.55 mmol, 1.2 equiv) in DMF (2 mL), and DIPEA (289 μL, 1.66 mmol, 3.6 equiv) was added to the reaction mixture. The yellow solution was stirred 7 h at RT. The reaction mixture was evaporated to obtain a brown oil, which was taken up in CH_2Cl_2 and washed four times with brine. The organic layer was dried over $MgSO_4$, filtered, and concentrated under vacuum. The oil was purified by flash-column chromatography (A: CH_2Cl_2, B: MeOH; with the following gradient program: 0% to 100% of B in 30 CV). An orange oil was obtained (110 mg, 33%, purity: 98%). RP-HPLC-MS: t_r = 4.55 min, m/z calculated for $C_{41}H_{53}N_5O_7$ $[M + H]^+$ 728.9, found 728.4. R_f (CH_2Cl_2/MeOH, 95/5) = 0.23. ^{1}H-NMR (500 MHz, $CDCl_3$): δ = 0.96 (s, 6H), 1.39 (t, J = 7.1 Hz, 3H), 2.00 (m, 2H), 2.06 (m, 2H), 2.71 (m, 1H), 2.76 (m, 2H), 2.90 (s, 3H), 2.93 (s, 3H), 3.12 (m, 5H), 3.38 (m, 2H), 3.55 (m, 2H), 3.63 (s, 6H), 4.41 (q, J = 7.1 Hz, 2H), 5.10 (s, 2H), 6.44 (d, J = 8.3 Hz, 2H), 6.92 (s, 1H), 7.2−7.4 (m, 9H) ppm. ^{13}C-NMR (126 MHz, $CDCl_3$): δ = 12.5 (CH_3), 14.4 (CH_3),

https://doi.org/10.1021/acs.jmedchem.1c00523
J. Med. Chem. 2021, 64, 8564−8578

21.8 (CH_2), 22.6 (CH_2), 25.4 (CH), 27.6 (CH_3), 34.3 (CH_3), 37.7 (CH_3), 39.4 (CH_3), 43.5 (CH_2), 44.4, 45.6 (CH_2), 50.8 (CH_3), 53.4, 53.8 (CH_2), 55.5 (CH_3), 60.9 (CH_2), 103.5 (CH), 106.5 (C), 111.2 (CH), 116.6 (CH), 124.3 (CH), 124.9 (CH), 127.7 (CH), 128.2 (CH), 128.6 (CH), 131.6 (C), 135.8 (C), 136.5 (C), 139.1 (C), 139.4 (C), 143.9 (C), 146.7 (C), 158.3 (C), 162.8 (C), 175.0 (C) ppm.

*1-(4-((3-((3-(((Benzyloxy)carbonyl)(methyl)amino)propyl)(methyl)amino)propyl)(methyl)carbamoyl)-2-isopropylphenyl)-5-(2,6-dimethoxyphenyl)-1H-pyrazole-3-carboxylic Acid (**8**).* To a solution of **7** (0.1 g, 0.14 mmol, 1 equiv) in dioxane (2 mL) was added a solution of 5 M KOH (0.274 mL, 1.4 mmol, 10 equiv). The yellow solution was stirred overnight at 40 °C. The reaction mixture was concentrated under vacuum. The residue was dissolved in water and acidified to a pH of 2 with 1 M HCl. The aqueous phase was extracted three times with CH_2Cl_2, dried over $MgSO_4$, filtered, and concentrated under vacuum to obtain a yellow oil (91 mg, 95%, purity: 98%). RP-HPLC-MS: t_r = 4.12 min, *m/z* calculated for $C_{39}H_{49}N_5O_7$ $[M + H]^+$ 700.3, found 700.3. ^{1}H-NMR (500 MHz, $CDCl_3$): δ = 0.96 (m, 6H), 2.03 (m, 4H), 2.69 (m, 1H), 2.77 (m, 2H), 2.90 (s, 3H), 2.93 (s, 3H), 3.0−3.2 (m, 5H), 3.4 (m, 2H), 3.5 (m, 2H), 3.6 (s, 6H), 5.11 (s, 2H), 6.44 (d, *J* = 8.3 Hz, 2H), 6.95 (s, 1H), 7.2−7.4 (m, 9H) ppm.

*2-(5-(2,6-Dimethoxyphenyl)-1-(2-isopropyl-4-(methyl-(3-(methyl-(3-(methylamino)propyl)amino)propyl)carbamoyl)phenyl)-1H-pyrazole-3-carboxamido)adamantane-2-carboxylic Acid (**9**).* To a solution of **8** (75 mg, 0.11 mmol, 1 equiv) in DMF (2 mL) was added NEt_3 (45 μL, 3.21 mmol, 3 equiv) and HATU (44.9 mg, 0.12 mmol, 1.1 equiv). The yellowish solution was stirred 20 min at RT. A solution of *tert*-butyl-2-aminoadamantane-2-carboxylate (synthon **D**) (29.7 mg, 0.12 mmol, 1.1 equiv) in DMF (1 mL) and NEt_3 (29.8 μL, 0.21 mmol, 2 equiv) was added, and the reaction mixture was stirred for 4 h at RT. The reaction mixture was concentrated under vacuum to obtain an orange oil. The intermediate was hydrogenated in EtOH (10 mL) and Pd/C 10% under atmospheric pressure of H_2. The suspension was stirred at RT for 2 days. The reaction mixture was filtered on celite and concentrated under vacuum to give an oil. Finally, CH_2Cl_2 (1 mL), TFA (1 mL), and H_2O (0.1 mL) were added. The yellow solution was stirred at RT for 1.5 h. The reaction mixture was concentrated under vacuum and purified by semi-preparative RP-HPLC on a BetaBasic-18 column (A: H_2O 0.1% TFA, B: MeCN 0.1% TFA with the following gradient program: 30% of B for 5 min, 30% to 60% of B in 50 min, at a flow rate of 20 mL/min) to obtain the product as a white powder (2 TFA salt, 29 mg, 27%, purity >99%). RP-HPLC-MS: t_r = 3.75 min, *m/z* calculated for $C_{42}H_{58}N_6O_6$ $[M + H]^+$ 743.4, found 743.3. ^{1}H-NMR (500 MHz, CD_3OD): δ = 1.10 (s, 6H), 1.65−1.90 (m, 9H), 2.0−2.25 (m, 9H), 2.64 (m, 2H), 2.73 (s, 3H), 2.80 (m, 1H), 2.94 (s, 3H), 2.97 (s, 3H), 3.12 (m, 4H), 3.27 (m, 2H), 3.68 (s, 6H), 6.57 (d, *J* = 8.5 Hz, 2H), 6.79 (s, 1H), 7.28 (t, *J* = 8.5 Hz, 1H), 7.37 (d, *J* = 8.1 Hz, 1H), 7.44 (s, 1H), 7.57 (s, 1H) ppm. ^{13}C-NMR (126 MHz, CD_3OD): δ = 18.4 (CH_3), 23.1 (CH_2), 23.9 (CH_2), 29.0 (CH_2), 29.3 (CH_2), 29.9 (CH), 34.5 (CH_2), 34.9 (CH_2), 35.0 (CH_2), 35.8 (CH_3), 39.0 (CH_2), 39.8 (CH_3), 41.2 (CH_3), 55.2 (CH_3), 57.1 (CH_2), 65.5 (CH_2), 106.6 (C), 110.8 (CH), 126.2 (CH), 127.1 (CH), 130.2 (CH), 133.8 (C), 138.8 (C), 148.3 (C), 160.7 (C), 176.3 (C) ppm. HRMS: *m/z* calculated for $C_{42}H_{58}N_6O_6$ $[M + H]^+$ 743.44972, found 743.44937; *m/z* calculated for $[M + 2H]^{2+}$ 372.22883, found 372.22752.

2-((1-(4-((3-((3-(DOTA-methylamino)propyl)methylamino)propyl)methylcarbamoyl)-2-isopropylphenyl)-5-(2,6-dimethoxyphenyl)-1H-pyrazole-3-carbonyl)amino)adamantane-2-carboxylic Acid (3BP-227). To a solution of **9** (TFA salt) (17 mg, 19.8 μmol, 1 equiv) in anhydrous DMF (1 mL) and DIPEA (10.3 μL, 59.4 μmol, 3 equiv) was added a solution of DOTA-NHS (30.16 mg, 39.6 μmol, 2 equiv) in anhydrous DMF (1 mL) with DIPEA (41.5 μL, 0.24 mmol, 12 equiv). The reaction mixture was stirred overnight at RT. The reaction medium was concentrated under vacuum, and the resulting oil was purified on a BetaBasic-18 column (A: H_2O 0.1% TFA, B: MeCN 0.1% TFA with the following gradient program: 30% of B for 5 min, 30% to 60% of B in 50 min, at a flow rate of 20 mL/min). The product 3BP-227 was obtained as a white powder (4 TFA salt, 22.8 mg, 73%, purity: 99%). RP-HPLC-MS: t_r = 3.88 min, *m/z* calculated for $C_{58}H_{84}N_{10}O_{13}$ $[M + H]^+$ 1129.6, found 1129.8. HRMS: *m/z* calculated for $C_{58}H_{84}N_{10}O_{13}$ $[M + H]^+$ 1129.62987, found 1129.63250.; *m/z* calculated for $[M + 2H]^{2+}$ 565.30309, found 565.31998.

Experimental Procedures and Characterization Data for Synthon C. *tert-Butyl (3-((2-Nitrophenyl)sulfonamido)propyl)-carbamate (**10**).* A solution of *N*-Boc-1,3-propanediamine (0.5 g, 2.87 mmol, 1 equiv), CH_2Cl_2 (7 mL), and triethylamine (0.4 mL, 2.87 mmol, 1 equiv) was cooled in an ice-water bath. 2-Nitrobenzenesulfonyl chloride (0.636 g, 2.87 mmol, 1 equiv) was added over a period of 5 min. After 5 min, the ice bath was removed and the reaction mixture was allowed to warm to room temperature and stirred for 15 min. The reaction mixture was extracted with CH_2Cl_2 and washed three times with a solution of citric acid (pH = 3). The organic layer was dried over $MgSO_4$, filtered, and concentrated under vacuum. The yellowish oil was purified by flash-column chromatography (A: CH_2Cl_2, B: CH_2Cl_2/MeOH 9:1; with the following gradient program: 100% to 0% of A in 20 CV). An oil, which crystallizes, was obtained (0.942 g, 90%, purity: 98%). RP-HPLC-MS: t_r = 4.46 min, *m/z* calculated for $C_{14}H_{21}N_3O_6S$ $[M + H]^+$ 360.1, found 260.1 $[M - Boc + H]^+$. R_f (CH_2Cl_2/MeOH, 9/1) = 0.68. ^{1}H-NMR (500 MHz, $CDCl_3$): δ = 1.42 (s, 9H), 1.69 (quint, *J* = 6.4 Hz, 2H), 3.15 (q, *J* = 6.4 Hz, 2H), 3.21 (q, *J* = 6.4 Hz, 2H), 4.67 (br, 1H), 5.87 (br, 1H), 7.72 (m, 2H), 7.84 (m, 1H), 8.16 (m, 1H) ppm; ^{13}C-NMR (126 MHz, $CDCl_3$): δ = 28.4 (CH_3), 30.6 (CH_2), 37.2 (CH_2), 40.8 (CH_2), 125.3 (CH), 130.9 (CH), 132.7 (CH), 133.4 (CH) ppm. (Note: three quaternary carbons not detected).

*tert-Butyl (3-((N-(3-(Dimethylamino)propyl)-2-nitrophenyl)-sulfonamido)propyl)carbamate (**11**).* To a solution of *tert*-butyl (3-((2-nitrophenyl)sulfonamido)propyl)carbamate (**10**) (0.94 g, 2.6 mmol, 1 equiv) in DMF (10 mL) was added K_2CO_3 (1.08 g, 7.8 mmol, 3 equiv). To the stirred suspension was added 3-dimethylamino-1-propyl hydrochloride (0.45 g, 2.86 mmol, 1.1 equiv) over a period of 5 min. The resulting suspension was heated to 60 °C overnight. The reaction mixture was cooled to RT, diluted with water (50 mL), and extracted three times with CH_2Cl_2. The organic layers were combined, washed with brine, dried over $MgSO_4$, filtered, and concentrated under vacuum. A yellowish oil (1.15 g, 99%, purity: 96%) was obtained. RP-HPLC-MS: t_r = 3.6 min, *m/z* calculated for $C_{19}H_{32}N_4O_6S$ $[M + H]^+$ 445.2, found 445.2. ^{1}H-NMR (500 MHz, $CDCl_3$): δ = 1.41 (s, 9H), 1.66 (quint, *J* = 6.9 Hz, 2H), 1.74 (quint, *J* = 6.9 Hz, 2H), 2.13 (s, 6H), 2.19 (t, *J* = 7.0 Hz, 2H), 3.14 (m, 2H), 3.32 (t, *J* = 7.4 Hz, 2H), 3.36 (t, *J* = 7.4 Hz, 2H), 4.91 (br, 1H), 7.62 (m, 2H), 7.98 (m, 2H) ppm; ^{13}C-NMR (126 MHz, $CDCl_3$): δ = 26.5 (CH_2), 28.4 (CH_3), 37.3 (CH_2), 45.3 (CH_2), 45.4 (CH_3), 45.9 (CH_2), 56.5 (CH_2), 79.2 (C), 124.2 (CH), 130.6 (CH), 131.7 (CH), 133.4 (CH), 133.5 (C), 148.1 (C), 156.0 (C) ppm.

*tert-Butyl (3-((3-(Dimethylamino)propyl)amino)propyl)-carbamate (Synthon **C**).* To a solution of *tert*-butyl (3-((*N*-(3-(dimethylamino)propyl)-2-nitrophenyl)sulfonamido)propyl)-carbamate (**11**) (1.1 g, 2.5 mmol, 1 equiv) in DMF (10 mL) was added cesium carbonate (3.3 g, 10 mmol, 4 equiv). Thiophenol (0.51 mL, 5 mmol, 2 equiv) was then added to the suspension, and the reaction mixture was stirred at 40 °C for 5 h. The reaction medium was extracted in a solution of citric acid (pH = 3) and washed three times with CH_2Cl_2. After basification with a solution of K_2CO_3, the compound was extracted four times with CH_2Cl_2. The organic layers were combined, dried over $MgSO_4$, filtered, and concentrated under vacuum. The yellowish oil was purified by semi-preparative HPLC on a BetaBasic-18 column (A: H_2O 0.1% TFA, B: MeCN 0.1% TFA; with the following gradient program: 0% of B for 10 min, 0% to 40% of B in 50 min, at a flow rate of 20 mL/min) to obtain a white solid as 3 TFA salt (0.681 g, 56%). RP-HPLC-MS: t_r = injection peak, *m/z* calculated for $C_{13}H_{29}N_3O_2$ $[M + H]^+$ 260.2, found 260.3. ^{1}H-NMR (500 MHz, DMSO-d_6): δ = 1.38 (s, 9H), 1.70 (quint, *J* = 7.8 Hz, 2H), 1.95 (quint, *J* = 7.8 Hz, 2H), 2.78 (s, 6H), 2.89 (m, 2H), 2.96 (m, 2H), 2.99 (m, 2H), 3.11 (m, 2H) ppm; ^{13}C-NMR (126 MHz, DMSO-d_6): δ = 21.3 (CH_2), 26.7 (CH_2), 28.8 (CH_3), 37.5 (CH_2), 42.7 (CH_2), 44.3 (CH_3), 45.2 (CH_2), 54.2 (CH_2), 78.3 (C) ppm (Note: one quaternary carbon not detected).

Experimental Procedures and Characterization Data for 12. *Ethyl 1-(4-((3-((tert-Butoxycarbonyl)amino)propyl)(3-(dimethylamino)propyl)carbamoyl)-2-isopropylphenyl)-5-(2,6-di-*

https://doi.org/10.1021/acs.jmedchem.1c00523
J. Med. Chem. 2021, 64, 8564−8578

*methoxyphenyl)-1H-pyrazole-3-carboxylate (**12**).* To a solution of **11** (0.4 g, 0.91 mmol, 1 equiv) in anhydrous DMF (5 mL) was added DIPEA (0.174 mL, 1.0 mmol, 1.1 equiv) and HATU (0.38 g, 1.0 mmol, 1.1 equiv). The orange solution was stirred 10 min at RT. A solution of *tert*-butyl (3-((3-(dimethylamino)propyl)amino)propyl)carbamate (2 TFA) (synthon **C**) (0.487 g, 1.0 mmol, 1.1 equiv) in DMF (5 mL) and DIPEA (0.522 mL, 3.0 mmol, 3.3 equiv) was added to the reaction mixture. The orange solution was stirred for 6 h at RT. The reaction mixture was evaporated to obtain an orange oil, which was taken up in CH_2Cl_2 and washed twice with brine. The organic layer was dried over $MgSO_4$, filtered, and concentrated under vacuum. An orange oil was obtained, which was purified by flash-column chromatography (A: CH_2Cl_2, B: MeOH; with the following gradient program: 100% to 70% of B in 30 CV). The product was isolated as an orange oil (0.602 g, 97%, purity: 96%). RP-HPLC-MS: t_r = 4.27 min, *m*/*z* calculated for $C_{37}H_{53}N_5O_7$ $[M + H]^+$ 680.4, found 680.5. ^{1}H-NMR (500 MHz, $CDCl_3$): δ = 0.98 (s, 6H), 1.39 (s, 9 H), 1.41 (t, *J* = 7.1 Hz, 3H), 1.68 (m, 2H), 1.81 (m, 1H), 2.04 (m, 1H), 2.19 (m, 2H), 2.72 (m, 1H), 2.79 (s, 6H), 3.1−3.3 (m, 4H), 3.55 (m, 2H), 3.65 (s, 6H), 4.42 (q, *J* = 7.1 Hz, 2H), 4.81 (br, 1H), 6.46 (d, *J* = 8.4 Hz, 2H), 6.92 (s, 1H), 7.16 (d, *J* = 7.8 Hz, 1H), 7.2−7.25 (m, 2H), 7.39 (d, *J* = 7.8 Hz, 1H) ppm. ^{13}C-NMR (126 MHz, $CDCl_3$): δ = 12.2 (CH_3), 14.5 (CH_3), 17.4 (CH), 18.6 (CH_2), 27.6 (CH_3), 28.4 (CH_3), 42.3 (CH_2), 43.1 (CH_3), 43.6 (CH_3), 54.2 (CH_3), 55.5 (CH_2), 60.9 (CH_2), 81.5 (CH), 103.5 (CH), 111.1 (CH), 124.2 (CH), 128.8 (CH), 131.6 (CH), 133.9 (CH), 158.3 (C), 162.7 (C) ppm.

Experimental Procedures and Characterization Data for Synthon D. *2-Aminoadamantane-2-carbonitrile (**13**).* A mixture of 2-adamantanone (2 g, 13.3 mmol, 1 equiv), NaCN (0.784 g, 16 mmol, 1.2 equiv), aqueous ammonia 25% solution (2.4 mL), and ammonium chloride (1.423 g, 26.6 mmol, 2 equiv) was dissolved in water (12 mL) and EtOH (24 mL). The resulting solution was stirred at 50 °C overnight. The solution was cooled to RT, extracted with Et_2O (120 mL), and concentrated. The white solid obtained was then purified on a silica plug (heptane/EtOAc 7:3). A white powder (2.16 g, 92%) was obtained. RP-HPLC-MS: t_r = 4.9 min, *m*/*z* calculated for $C_{11}H_{16}N_2$ $[M + H + MeCN]^+$ 218.1, found 218.1. R_f (heptane/EtOAc, 7/3) = 0.4. ^{1}H-NMR (500 MHz, $CDCl_3$): δ = 1.54 (m, 1H), 1.70 (m, 1H), 1.72 (m, 1H), 1.76 (m, 1H), 1.84 (m, 1H), 1.87 (m, 1H), 1.90 (m, 1H), 1.93 (m, 1H), 1.96 (m, 1H), 1.98 (m, 1H), 2.06 (m, 1H), 2.14 (m, 1H), 2.23 (d, 1H), 2.51 (m, 1H) ppm; ^{13}C-NMR (126 MHz, $CDCl_3$): δ = 26.5 (CH), 26.8 (CH), 27.5 (CH), 30.3 (CH_2), 35.0 (CH_2), 36.4 (CH_2), 36.6 (CH), 37.6 (CH_2), 39.3 (CH_2), 56.4 (C), 125.5 (C) ppm. mp: 186 °C.

*N-(2-Cyanoadamantan-2-yl)benzamide (**14**).* To a solution of 2-aminoadamantane-2-carbonitrile (**13**) (1.5 g, 8.5 mmol, 1 equiv) in THF (15 mL) was added a solution of K_2CO_3 (1.78 g, 12.9 mmol, 1.52 equiv) in water (15 mL). To the resulting solution was added dropwise, over 30 min, a solution of benzoyl chloride (1.48 mL, 12.8 mmol, 1.5 equiv) in THF (15 mL) with vigorous stirring at RT. After 5 min, a white precipitate began to form. After a further 2 h, the white solid was isolated by filtration and dried under vacuum. The solid was purified on a silica plug (CH_2Cl_2/MeOH 95:5) to obtain a white powder (1.64 g, 69%, purity: 90%). RP-HPLC-MS: t_r = 4.79 min, *m*/*z* calculated for $C_{18}H_{20}N_2O$ $[M + H]^+$ 281.2, found 281.1. R_f (heptane/EtOAc, 7/3) = 0.31. ^{1}H-NMR (500 MHz, $CDCl_3$): δ = 1.76 (m, 3H), 1.85−2.02 (m, 8H), 2.05 (m, 1H), 2.32 (d, 1H), 2.65 (m, 1H), 6.12 (br, 1H), 7.43 (td, *J* = 8.5, 1.7 Hz, 2H), 7.52 (tt, *J* = 8.5, 1.7 Hz, 1H), 7.77 (dt, *J* = 8.5, 1.7 Hz, 2H) ppm; ^{13}C-NMR (126 MHz, $CDCl_3$): δ = 26.2 (CH), 26.5 (CH), 27.6 (CH_2), 31.5 (CH_2), 33.9 (CH), 34.2 (CH_2), 37.3 (CH_2), 39.4 (CH_2), 47.1 (CH), 57.3 (C), 120.2 (C), 127.2 (CH), 128.9 (CH), 132.3 (CH), 134.0 (C), 166.6 (C) ppm. mp: 250 °C.

*2-Aminoadamantane-2-carboxylic Acid Hydrochloride (**15**).* To *N*-(2-cyanoadamantan-2-yl)benzamide (**14**) (1 g, 3.6 mmol, 1 equiv) was added acetic acid (18 mL), concentrated HCl (5 mL), and water (3 mL). The white suspension was then heated to reflux for 5 days. The reaction mixture was concentrated under vacuum to obtain a white solid, which was triturated twice in hot Et_2O (40 mL) and twice in hot MeCN (25 mL). A white powder (0.768 g, 92%) was obtained. RP-HPLC-MS: t_r = 0.5 min, *m*/*z* calculated for $C_{11}H_{17}NO_2$ $[M + H]^+$ 196.1, found 196.3. ^{1}H-NMR (500 MHz, DMSO-d_6): δ = 1.6−2.2 (m, 14H), 8.59 (br, 2H), 13.84 (br, 1H) ppm; ^{13}C-NMR (126 MHz, DMSO-d_6): δ = 26.2 (CH), 31.2 (CH_2), 32.2 (CH), 34.4 (CH_2), 37.5 (CH_2), 63.9 (C), 171.4 (C) ppm. mp: 271 °C.

*tert-Butyl 2-Aminoadamantane-2-carboxylate (Synthon **D**).* A suspension of 2-aminoadamantane-2-carboxylic acid hydrochloride (**15**) (0.7 g, 3.0 mmol, 1 equiv) in *tert*-butyl acetate (25 mL) was cooled to 0 °C. $HClO_4$ (0.42 mL, 4.8 mmol, 1.6 equiv) was added dropwise, and the reaction mixture was stirred at RT overnight. A 2 M NaOH (40 mL) solution was added slowly at 0 °C to quench the reaction until the pH reached 9−10. The mixture was then extracted with EtOAc (4 × 100 mL) and washed with brine. After being dried with $MgSO_4$, the organic layer was filtered and concentrated under vacuum to obtain a white solid, which was purified by flash-column chromatography (A: CH_2Cl_2, B: CH_2Cl_2/MeOH 9:1; with the following gradient program: 0% to 20% of B in 10 CV, 20% of B for 10 CV). A white solid (0.3 g, 40%, purity: 96%) was obtained. RP-HPLC-MS: t_r = 3.7 min, *m*/*z* calculated for $C_{15}H_{25}NO_2$ $[M + H]^+$ 252.2, found 252.2. R_f (CH_2Cl_2/MeOH, 98/2) = 0.34. ^{1}H-NMR (500 MHz, $CDCl_3$): δ = 1.35 (m, 2H), 1.40 (s, 9H), 1.47 (m, 2H), 1.60 (m, 2H), 1.69 (m, 6H), 1.97 (m, 2H), 2.15 (m, 2H) ppm; ^{13}C-NMR (126 MHz, $CDCl_3$): δ = 26.9 (CH), 27.2 (CH_3), 27.9 (CH), 32.0 (CH_2), 34.1 (CH), 35.1 (CH_2), 37.8 (CH_2), 61.8 (C), 79.9 (C), 176.0 (C) ppm. mp: 99 °C.

Experimental Procedures and Characterization Data for Precursor 16. *2-((1-(4-((3-Aminopropyl)-(3-dimethylaminopropyl)-carbamoyl)-2-isopropylphenyl)-5-(2,6-dimethoxyphenyl)-1H-pyrazole-3-carbonyl)amino)adamantane-2-carboxylic acid (**16**).* To a solution of **12** (0.602 g, 0.86 mmol, 1 equiv) in dioxane (9 mL) was added a solution of 5 M KOH (0.886 mL, 4.43 mmol, 5 equiv). The yellow solution was stirred overnight at RT. The reaction mixture was concentrated under vacuum. The residue was taken up in water and washed three times with Et_2O. The aqueous phase was acidified to pH 3−4 (precipitation) with a solution of 1 M HCl and evaporated. EtOH was added to the residue and KCl was filtered off. The solution was concentrated under vacuum to obtain an orange oil. DMF (15 mL), NEt_3 (0.46 mL, 3.3 mmol, 3 equiv), and HATU (0.46 g, 1.2 mmol, 1.1 equiv) were added. The yellowish solution was stirred for 15 min at RT. A solution of *tert*-butyl-2-aminoadamantane-2-carboxylate (synthon **D**) (0.302 g, 1.2 mmol, 1.1 equiv) in DMF (5 mL) and NEt_3 (0.31 mL, 2.2 mmol, 2 equiv) was added to the reaction mixture and stirred for 4 h at RT. The reaction mixture was concentrated under vacuum to obtain an orange oil. Finally, CH_2Cl_2 (5 mL), TFA (5 mL), and H_2O (0.5 mL) were added. The yellow solution was stirred at RT for 1.5 h. The reaction mixture was concentrated under vacuum and purified by semi-preparative HPLC on a BetaBasic-18 column (A: H_2O 0.1% TFA, B: MeCN 0.1% TFA with the following gradient program: 20% of b for 5 min, 20% to 60% of B in 50 min, at a flow rate of 20 mL/min) to obtain **16** as a white powder (2 TFA salt, 0.456 g, 55%, purity: 99%). RP-HPLC-MS: t_r = 3.66 min, *m*/*z* calculated for $C_{41}H_{56}N_6O_6$ $[M + H]^+$ 729.4, found 729.3. ^{1}H-NMR (500 MHz, $CDCl_3$): δ = 0.97 (s, 6H), 1.49 (m, 2H), 1.63 (m, 4H), 1.67−1.80 (m, 4H), 1.90 (m, 2H), 1.98 (m, 2H), 2.11 (m, 4H), 2.51 (m, 2H), 2.6−2.7 (m, 2H), 2.72 (s, 3H), 2.78 (m, 1H), 2.91 (s, 3H), 3.09 (m, 1H), 3.2−3.35 (m, 3H), 3.57 (s, 6H), 6.6 (d, *J* = 8.4 Hz, 2H), 6.87 (s, 1H), 7.2−7.4 (m, 4H) ppm. ^{13}C-NMR (126 MHz, $CDCl_3$): δ = 11.3 (CH_3), 26.4 (CH_3), 27.6 (CH_3), 33.4 (CH_2), 36.7 (CH_2), 37.0 (CH_2), 42.6 (CH_3), 42.8 (CH_3), 54.5 (CH_2), 55.2 (CH_2), 55.6 (CH_3), 63.6 (CH_2), 104.0 (CH), 105.6 (C), 109.0 (CH), 123.5 (CH), 124.3 (CH), 129.9 (CH), 137.8 (C), 158.1 (C), 159.4 (C) ppm. HRMS: *m*/*z* calculated for $C_{41}H_{56}N_6O_6$ $[M + H]^+$ 729.43407, found 729.43468; *m*/*z* calculated for $[M + Na]^+$ 751.41590, found 751.41378.

General Procedure for the Coupling of the Chelating Agent. To a solution of **16** (1 equiv) in anhydrous DMF (0.5 mL) and DIPEA (2 equiv) was added a solution of the chelating agent (1.5 equiv) in anhydrous DMF (0.5 mL) with DIPEA (6−9 equiv depending on the chelator). The reaction mixture was stirred for 2−4 h at RT until completion. The reaction medium was concentrated under vacuum, and the oil was purified on a semi-preparative column.

2-((1-(4-((3-DOTA-aminopropyl)-(3-dimethylaminopropyl)-carbamoyl)-2-isopropylphenyl)-5-(2,6-dimethoxyphenyl)-1H-pyra-

https://doi.org/10.1021/acs.jmedchem.1c00523
J. Med. Chem. 2021, 64, 8564−8578

zole-3-carbonyl)amino)adamantane-2-carboxylic Acid (3BP-228). Chelator: DOTA-NHS, Reaction time: 2 h, Equiv. DIPEA: 9. Purification on a BetaBasic-18 column (A: H_2O 0.1% TFA, B: MeCN 0.1% TFA with the following gradient program: 20% of B for 5 min, 20% to 60% of B in 45 min, at a flow rate of 20 mL/min). The product 3BP-228 was obtained as a white powder (3 TFA salt, 21 mg, 40%, purity: 93%). RP-HPLC-MS: t_r = 3.83 min, *m/z* calculated for $C_{57}H_{82}N_{10}O_{13}$ $[M + H]^+$ 1115.6, found 1115.7. HRMS: *m/z* calculated for $C_{57}H_{82}N_{10}O_{13}$ $[M + H]^+$ 1115.61422, found 1115.61484; *m/z* calculated for $[M + Na]^+$ 1137.59605, found 1139.59447.

*2-((1-(4-((3-DOTAGA-aminopropyl)-(3-dimethylaminopropyl)-carbamoyl)-2-isopropylphenyl)-5-(2,6-dimethoxyphenyl)-1H-pyrazole-3-carbonyl)amino)adamantane-2-carboxylic Acid (DOTAGA-**16**).* Chelator: DOTAGA anhydride, Reaction time: 4 h, Equiv. DIPEA: 6. Purification on a BetaBasic-18 column (A: H_2O 0.1% TFA, B: MeCN 0.1% TFA with the following gradient program: 30% of B for 5 min, 30% to 70% of B in 50 min, at a flow rate of 20 mL/min). The product DOTAGA-**16** was obtained as a white powder (4 TFA salt, 21.59 mg, 37%, purity: 97%). RP-HPLC-MS: t_r = 3.82 min, *m/z* calculated for $C_{60}H_{86}N_{10}O_{15}$ $[M + H]^+$ 1187.6, found 1187.6. HRMS: *m/z* calculated for $C_{60}H_{86}N_{10}O_{15}$ $[M + H]^+$ 1187.63535, found 1187.63587; *m/z* calculated for $[M + 2H]^{2+}$ 594.32165, found 594.32077.

*2-((1-(4-((3-NOTA-aminopropyl)-(3-dimethylaminopropyl)-carbamoyl)-2-isopropylphenyl)-5-(2,6-dimethoxyphenyl)-1H-pyrazole-3-carbonyl)amino)adamantane-2-carboxylic Acid (NOTA-**16**).* Chelator: NOTA-NHS, Reaction time: 3 h, Equiv. DIPEA: 7.5. Purification on a BetaBasic-18 column (A: H_2O 0.1% TFA, B: MeCN 0.1% TFA with the following gradient program: 30% of B for 5 min, 30% to 60% of B in 50 min, at a flow rate of 20 mL/min). The product NOTA-**16** was isolated as a white powder (3 TFA salt, 14.39 mg, 30%, purity: 98%). RP-HPLC-MS: t_r = 3.85 min, *m/z* calculated for $C_{53}H_{75}N_9O_{11}$ $[M + H]^+$ 1014.6, found 1014.6. HRMS: *m/z* calculated for $C_{53}H_{75}N_9O_{11}$ $[M + H]^+$ 1014.56654, found 1014.56629.

*2-((1-(4-((3-NODAGA-aminopropyl)-(3-dimethylaminopropyl)-carbamoyl)-2-isopropylphenyl)-5-(2,6-dimethoxyphenyl)-1H-pyrazole-3-carbonyl)amino)adamantane-2-carboxylic Acid (NODAGA-**16**).* Chelator: NODAGA-NHS, Reaction time: 2 h, Equiv. DIPEA: 8. Purification on a BetaBasic-18 column (A: H_2O 0.1% TFA, B: MeCN 0.1% TFA with the following gradient program: 30% of B for 5 min, 30% to 70% of B in 50 min, at a flow rate of 20 mL/min). The product NODAGA-**16** was obtained as a white powder (4 TFA salt, 35.89 mg, 65%, purity: 96%). RP-HPLC-MS: t_r = 3.9 min, *m/z* calculated for $C_{56}H_{79}N_9O_{13}$ $[M + H]^+$ 1086.6, found 1086.7. HRMS: *m/z* calculated for $C_{56}H_{79}N_9O_{13}$ $[M + H]^+$ 1086.58767, found 1086.58672; *m/z* calculated for $[M + 2H]^{2+}$ 543.79781, found 543.79634.

*2-((1-(4-((3-THP-aminopropyl)-(3-dimethylaminopropyl)-carbamoyl)-2-isopropylphenyl)-5-(2,6-dimethoxyphenyl)-1H-pyrazole-3-carbonyl)amino)adamantane-2-carboxylic Acid (THP-**16**).* Chelator: THP-NCS, Reaction time: 4 h, Equiv. DIPEA: 9. Purification on a BetaBasic-18 column (A: H_2O 0.1% TFA, B: MeCN 0.1% TFA with the following gradient program: 30% of B for 5 min, 30% to 60% of B in 50 min, at a flow rate of 20 mL/min). The product THP-**16** was obtained as a white powder (7 TFA salt, 13.6 mg, 46%, purity: 97%, the peak at 3.8 min corresponds to the expected compound, and the peak at 4.1 min corresponds to an Fe adduct formed during the analysis). RP-HPLC-MS: t_r = 3.84 min, *m/z* calculated for $C_{86}H_{112}N_{16}O_{16}S_2$ $[M + 2H]^{2+}$ 845.4, found 845.7. HRMS: *m/z* calculated for $C_{56}H_{79}N_9O_{13}$ $C_{86}H_{112}N_{16}O_{16}S_2$ $[M + 2H]^{2+}$ 845.38630, found 845.40299; *m/z* calculated for $[M + 3H]^{3+}$ 563.93739, found 564.26978.

Experimental Procedures and Characterization Data for bisDOTAGA-16. *Lys(DOTAGA(tBu)$_4$)$_2$.* To a solution of DOTAGA-(tBu)$_4$ (40 mg, 57 μmol, 1.9 equiv) in anhydrous DMF (1 mL) with DIPEA (21 μL, 120 μmol, 4 equiv) was added HATU (21.7 mg, 57 μmol, 1.9 equiv). The yellow solution was stirred for 15 min at RT, and DIPEA (21 μL, 120 μmol, 4 equiv) and L-lysine monochlorohydrate (5.5 mg, 30 mmol, 1 equiv) were added. The reaction mixture was stirred for 4 h at RT. The reaction medium was concentrated under vacuum and purified on a BetaBasic-18 column (A: H_2O 0.1% TFA, B: MeCN 0.1% TFA with the following gradient program: 20% of B for 5 min, 20% to 80% of B in 70 min, at a flow rate of 20 mL/min). The product was obtained as a white powder (4 TFA salt, 25.8 mg, 44%, purity: 90%). RP-HPLC-MS: t_r = 3.88 min, *m/z* calculated for $C_{76}H_{138}N_{10}O_{20}$ $[M + 1H]^{1+}$ 1512.01, found 1512.1; $[M + 2H]^{2+}$ 756.5, found 756.5. HRMS: *m/z* calculated for $C_{76}H_{138}N_{10}O_{20}$ $[M + H]^+$ 1512.01683, found 1512.01873; *m/z* calculated for $[M + 2H]^{2+}$ 756.51239, found 756.51434.

*BisDOTAGA-**16**.* To a solution of Lys(DOTAGA(tBu)$_4$)$_2$ (15.7 mg, 10.4 μmol, 1 equiv) in anhydrous DMF (0.5 mL) was added DIPEA (5.4 μL, 31.2 μmol, 3 equiv) and then HATU (3.95 mg, 10.4 μmol, 1 equiv). The solution was stirred 15 min at RT, and a solution of **16** (8.77 mg, 10.4 μmol, 1 equiv) in anhydrous DMF (0.5 mL) with DIPEA (7.3 μL, 41.6 μmol, 4 equiv) was added. The reaction mixture was stirred 5 h at RT. The reaction medium was concentrated under vacuum, and a solution of TFA:triisopropylsilane:H_2O (95:2.5:2.5, v/v/v, 2 mL) was added. The reaction was stirred for 3 h at 45 °C and concentrated under a flow of nitrogen gas. The solution was purified on a BetaBasic-18 column (A: H_2O 0.1% TFA, B: MeCN 0.1% TFA with the following gradient program: 20% of B for 5 min, 20% to 60% of B in 60 min, at a flow rate of 20 mL/min). The product bisDOTAGA-**16** was obtained as a white powder (4 TFA salt, 7.94 mg, 34%, purity: 97%). RP-HPLC-MS: t_r = 3.73 min, *m/z* calculated for $C_{85}H_{128}N_{16}O_{25}$ $[M + 2H]^{2+}$ 887.5, found 888.2; $[M + 3H]^{3+}$ 592.0, found 592.5. HRMS: *m/z* calculated for $C_{85}H_{128}N_{16}O_{25}$ $[M + 2H]^{2+}$ 887.46977, found 887.47499.

Experimental Procedures and Characterization Data for bisNODAGA-16. *Lys(NODAGA(tBu)$_3$)$_2$.* To a solution of NODAGA-(tBu)$_3$ (75 mg, 0.138 mmol, 2.5 equiv) in anhydrous DMF (1 mL) with DIPEA (47.9 μL, 0.275 mmol, 5 equiv) was added TSTU (50 mg, 0.165 mmol, 3 equiv). The yellow solution was stirred for 30 min at RT, and a suspension of L-lysine monochlorohydrate (10 mg, 0.055 mmol, 1 equiv) in DMF (1 mL) and DIPEA (28.7 μL, 0.165 mmol, 3 equiv) was added to the reaction mixture. The yellow suspension was stirred overnight at RT and heated for 4 h at 50 °C. The reaction medium was concentrated under vacuum and purified on a BetaBasic-18 column (A: H_2O 0.1% TFA, B: MeCN 0.1% TFA with the following gradient program: 25% of B for 5 min, 25% to 75% of B in 50 min, at a flow rate of 20 mL/min). The product was obtained as a white powder (3 TFA salt, 66.4 mg, 78%, purity: 92%). RP-HPLC-MS: t_r = 4.15 min, *m/z* calculated for $C_{60}H_{108}N_8O_{16}$ $[M + H]^+$ 1197.8, found 1197.8; *m/z* calculated for $[M + 2H]^{2+}$ 599.4, found 599.6. HRMS: *m/z* calculated for $C_{60}H_{108}N_8O_{16}$ $[M + H]^+$ 1197.79627, found 1197.79853; *m/z* calculated for $[M + 2H]^{2+}$ 599.40211, found 599.40336.

*BisNODAGA-**16**.* To a solution of Lys(NODAGA(tBu)$_3$)$_2$ (15 mg, 12.5 μmol, 1 equiv) in anhydrous DMF (0.75 mL) with DIPEA (6.5 μL, 37.5 μmol, 3 equiv) was added HATU (4.75 mg, 12.5 μmol, 1 equiv). The solution was stirred for 15 min at RT, and a solution of **16** (10.5 mg, 12.5 μmol, 1 equiv) in anhydrous DMF (0.75 mL) with DIPEA (8.7 μL, 50.0 μmol, 4 equiv) was added. The reaction mixture was left stirring for 3 h at RT. The reaction medium was concentrated under vacuum, and a solution of TFA:triisopropylsilane:H_2O (95:2.5:2.5, *v/v/v*, 2 mL) was added. The reaction was stirred for 6 h at RT and concentrated under a flow of nitrogen gas. The residue was purified on a BetaBasic-18 column (A: H_2O 0.1% TFA, B: MeCN 0.1% TFA with the following gradient program: 20% of B for 5 min, 20% to 60% of B in 40 min, at a flow rate of 20 mL/min). The product bisNODAGA-**16** was obtained as a white powder (4 TFA salt, 12.0 mg, 47%, purity: 98%). RP-HPLC-MS: t_r = 3.90 min, *m/z* calculated for $C_{77}H_{114}N_{14}O_{21}$ $[M + 2H]^{2+}$ 786.4, found 786.4. HRMS: *m/z* calculated for $C_{77}H_{114}N_{14}O_{21}$ $[M + H]^+$ 1571.83624, found 1571.83830; *m/z* calculated for $[M + 2H]^{2+}$ 786.42209, found 786.42406.

General Procedure for the Metalation with ^{nat}Ga. The compounds were dissolved in acetate buffer (0.5 mL, 0.1 M, pH 3.48). A solution of $Ga(NO_3)_3$ (1.5 equiv for 3BP-227, 3BP-228, DOTAGA-**16**, NOTA-**16**, NODAGA-**16**, and THP-**16** and 4 equiv for bisDOTAGA-**16** and bisNODAGA-**16**) in acetate buffer (0.5 mL) was then added. The reaction mixture was stirred for 5 h at 40 °C. The excess of free gallium was removed by semi-preparative RP-HPLC.

^{nat}Ga-3BP-227. Purification on a BetaBasic-18 column (A: H_2O 0.1% TFA, B: MeCN 0.1% TFA with the following gradient program: 30% of B for 5 min, 30% to 60% of B in 50 min, at a flow rate of 20 mL/min). The product was obtained as a white powder (5 TFA salt, 5.8 mg,

https://doi.org/10.1021/acs.jmedchem.1c00523
J. Med. Chem. 2021, 64, 8564−8578

49%, purity: 97%). RP-HPLC-MS: t_r = 3.85 min. MALDI-TOF: m/z calculated for $C_{58}H_{81}GaN_{10}O_{13}$ $[M + H]^+$ 1195.532, found 1195.703.

^{nat}Ga-3BP-228. Purification on a BetaBasic-18 column (A: H_2O 0.1% TFA, B: MeCN 0.1% TFA with the following gradient program: 30% of B for 5 min, 30% to 60% of B in 50 min, at a flow rate of 20 mL/min). The product was obtained as a white powder (3 TFA salt, 8.7 mg, 70%, purity: 97%). RP-HPLC-MS: t_r = 3.77 min. MALDI-TOF: m/z calculated for $C_{57}H_{79}GaN_{10}O_{13}$ $[M + H]^+$ 1181.516, found 1181.844.

*^{nat}Ga-DOTAGA-**16***. Purification on a BetaBasic-18 column (A: H_2O 0.1% TFA, B: MeCN 0.1% TFA with the following gradient program: 30% of B for 5 min, 30% to 60% of B in 50 min, at a flow rate of 20 mL/min). The product was obtained as a white powder (5 TFA salt, 7.1 mg, 51%, purity: 92%). RP-HPLC-MS: t_r = 3.87 min. MALDI-TOF: m/z calculated for $C_{60}H_{82}GaN_{10}O_{15}^-$ $[M + H]^+$ 1252.530, found 1253.844.

*^{nat}Ga-NOTA-**16***. Purification on a BetaBasic-18 column (A: H_2O 0.1% TFA, B: MeCN 0.1% TFA with the following gradient program: 25% of B for 5 min, 25% to 50% of B in 50 min, at a flow rate of 20 mL/min). The product was obtained as a white powder (3 TFA salt, 10.6 mg, 84%, purity: 99%). RP-HPLC-MS: t_r = 3.66 min. MALDI-TOF: m/z calculated for $C_{53}H_{73}GaN_9O_{11}^+$ $[M + H]^+$ 1081.476, found 1080.467.

*^{nat}Ga-NODAGA-**16***. Purification on a BetaBasic-18 column (A: H_2O 0.1% TFA, B: MeCN 0.1% TFA with the following gradient program: 30% of B for 5 min, 30% to 60% of B in 50 min, at a flow rate of 20 mL/min). The compound was obtained as a white powder (3 TFA salt, 4.35 mg, 35%, purity >99%). RP-HPLC-MS: t_r = 3.9 min. MALDI-TOF: m/z calculated for $C_{56}H_{76}GaN_9O_{13}$ $[M + H]^+$ 1152.490, found 1152.454.

*^{nat}Ga-THP-**16***. Purification on a BetaBasic-18 column (A: H_2O 0.1% TFA, B: MeCN 0.1% TFA with the following gradient program: 35% of B for 5 min, 35% to 60% of B in 40 min, at a flow rate of 20 mL/min). The product was obtained as a white powder (9 TFA salt, 6 mg, 53%, purity: 77 + 20%). RP-HPLC-MS: t_r = 4.2 min. MALDI-TOF: m/z calculated for $C_{86}H_{109}GaN_{16}O_{16}S_2$ $[M + H]^+$ 1755.698, found 1757.551.

*^{nat}Ga-bisDOTAGA-**16***. Purification on a BetaBasic-18 column (A: H_2O 0.1% TFA, B: MeCN 0.1% TFA with the following gradient program: 20% of B for 5 min, 20% to 60% of B in 40 min, at a flow rate of 20 mL/min). The product was obtained as a white powder (3 TFA salt, 5.44 mg, 78%, purity: 97.4%). RP-HPLC-MS: t_r = 3.73 min. MALDI-TOF: m/z calculated for $C_{85}H_{122}Ga_2N_{16}O_{25}$ $[M + H]^+$ 1907.735, found 1908.386.

*^{nat}Ga-bisNODAGA-**16***. Purification on a BetaBasic-18 column (A: H_2O 0.1% TFA, B: MeCN 0.1% TFA with the following gradient program: 20% of B for 5 min, 20% to 60% of B in 40 min, at a flow rate of 20 mL/min). The product was obtained as a white powder (3 TFA salt, 5.33 mg, 77%, purity: 96%). RP-HPLC-MS: t_r = 3.72 min. MALDI-TOF: m/z calculated for $C_{77}H_{108}Ga_2N_{14}O_{21}$ $[M + H]^+$ 1706.643, found 1706.394.

In Vitro Stability. Fifteen microliters of a 5 mM stock solution of compound in DMSO 50% (v/v) was stirred in a thermomixer (900 rpm, 37 °C, dark) with 135 μL of mouse serum (Sigma Aldrich, M5905, batch SLBT4412). The final concentration in peptide was 0.5 mM. After 0 min, 30 min, 1 h, 2 h, 4 h, and 24 h, a sample (15 μL) of solution was collected and diluted with 60 μL of ethanol 99%. Fifteen microliters of a 1 mM stock solution of Fmoc-Trp(*t*Bu)-OH was added to the suspension for internal calibration. Samples were vortexed and centrifuged (10,000 rpm, 10 min) to remove precipitated proteins. The supernatant was analyzed by RP-HPLC-MS at a wavelength of 260 nm.

***In Vitro* Binding Affinity.** The affinity of each compound Ga-3BP-227, Ga-3BP-228, Ga-DOTAGA-**16**, Ga-NOTA-**16**, Ga-NODAGA-**16**, Ga-THP-**16**, Ga-bisDOTAGA-**16**, and Ga-bisNODAGA-**16** for NTS_1 was determined on a competitive binding assay on human recombinant CHO cells overexpressing NTS_1, using [^{125}I]I-Tyr^3-neurotensin (0.05 nM; K_d = 0.22 nM) as the radioligand (Eurofins, France). Non-specific binding was measured in the presence of an excess of neurotensin (1 μM). Experiments were performed in duplicate. Data were fitted by non-linear regression, using GraphPad Prism 6.0 software. The minimum was set to 0. IC_{50} values were converted into inhibition constants (K_i) using the Cheng−Prusoff equation.

Radiolabeling of Compounds with ^{68}Ga. Compounds were radiolabeled using a Modular-Lab PharmTracer (Eckert & Ziegler). Fractional elution of the ^{68}Ge/^{68}Ga generator gave a solution (1.5 mL, 90 MBq), which was added to a solution of 2.99 nmol of each compound in EtOH (150 μL) and ammonium acetate buffer (1 M, pH 6.88) to adjust the pH to 3.5. The reaction mixture was incubated at 37 °C for 5 min for the NOTA-, NODAGA-, and THP-based compounds, and at 95 °C for 10 min for the DOTA- and DOTAGA-based compounds. The products were purified on a C_{18} Sep-Pack cartridge (Waters, Milford, MA), eluted using 1000 μL of 80% ethanol in the second reactor, and subsequently evaporated at 70 °C for 10 min under an air flow. The final products were diluted with 0.9% sodium chloride (NaCl). HPLC quality control was performed using a HPLC system LC-2000 analytical series (Jasco) equipped with a Flowcount radioactivity detector (Bioscan). Separation was achieved using an RP C_{18} Kinetex column (Phenomenex) (2.6 μm, 100 Å, 50 × 2.1 mm) with ultrapure water and HPLC-grade MeCN (A: H_2O 0.1% TFA and B: MeCN 0.1% TFA). Analyses were performed with the following gradient program: 5% to 95% of B in 5 min, 95% B for 1.5 min, at a flow rate of 0.5 mL/min. The quantity of colloids was evaluated using a system of two instant thin layer chromatographies (iTLC) eluted with citrate sodium and NH_4Ac/MeOH as mobile phases.

Small Animal PET Imaging and Biodistribution Studies on the HT29 Tumor Model. All animal studies were conducted at and approved by the Centre George François Leclerc (CGFL) in accordance with the relevant guidelines and legislation on the use of laboratory animals (directive 2010/63/EU) and were approved by the accredited Ethical Committee (C2ea Grand Campus no. 105) and French Ministry of Higher Education and Research (#15316). HT-29 tumor bearing mice (8 weeks old, 10×10^6 cells per mouse injected subcutaneously in the right flack) were intravenously injected in the tail vein with 3−8 MBq of each radiotracer based on a consistent number of picomoles being injected (500 pmol). Static PET and MRI images were simultaneously recorded 90 min p.i. for 30 min. The mice were awakened between the administration of the tracer and imaging times. Images were recorded in a dual-ring SiPM microPET fully integrated in a 7T preclinical MRI (MR Solutions, Guilford, UK). The animals were kept under anesthesia using 2% isofluorane in oxygen and positioned in a dedicated heating cradle during imaging. Respiratory gating was performed with abdominal pressure sensor and dedicated software (PC Sam, SAII, Stony Brook, US). List-mode data were collected in the PET system during 30 min. Coronal T1 weighted fast spin echo MR images were acquired with respiratory gating and the following parameters: 16 slices with a time of repetition (TR) of 1000 ms, time of echo (TE) of 11 ms, 3 signal averages, 1 mm slice thickness, field of view (FOV) of 70 mm, and 256 × 256 pixel matrix. Images were reconstructed with the 3D ordered subset expectation maximization (OSEM) algorithm implemented in the system using 2 iterations, 32 subsets, and an isotropic voxel size of 0.28 mm. An energy window of 250−750 keV and a coincidence time window of 8 ns were applied to the list-mode data. The algorithm takes into account normalization, random, and decay corrections. No attenuation correction was applied. Two hours post-injection, mice were sacrificed and the main organs and tissues were dissected, weighed, and γ-counted (1480 Wizard 3, PerkinElmer). Blocking experiments were performed by co-injecting an excess (100 equivalents) of SR142948A. Tumor or tissue uptake are expressed as mean ± SD percentage injected dose per gram (%ID/g), corrected for radionuclide decay. Statistical significance between different groups was analyzed by the one-way analysis of variance, with [^{68}Ga]Ga-3BP-228 as a control group, followed by Bonferroni correction. Statistical significance in blocking experiments was assessed by the unpaired two-tailed Student's *t*-test.

Binding Studies on HT29 Cells. Experiments were performed with 1×10^6 cells per well in 24-well plates. Cells were washed with ice cold PBS twice before their incubation with 8 different concentrations of [^{68}Ga]Ga-bisNODAGA-**16** (from 78 pM to 10 nM) in 1 mL of incubation medium. The compound was incubated alone or in the presence of an excess (1 μM) of the ligands SR142948A, neurotensin, or levocabastine, for 60 min at 4 °C. The medium was then withdrawn, cells were washed twice with ice-cold PBS and solubilized in 1 M

https://doi.org/10.1021/acs.jmedchem.1c00523
J. Med. Chem. 2021, 64, 8564−8578

NaOH. The amount of radioactivity was measured using a γ-counter (Wallac Wizard 1470, Perkin Elmer, USA). Experiments were performed in triplicate. Data were fitted, using GraphPad Prism 6.0 software, by applying the one site binding model.

Calcium Mobilization Assay. Antagonist activities were determined on a fluorescence assay measuring $[Ca^{2+}]$ mobilization in CHO cells overexpressing human recombinant NTS_1, upon stimulation by neurotensin (0.3 nM), in the presence of increasing concentrations of ^{nat}Ga-bisNODAGA-**16** (Eurofins, France).[19] SR142948A was used as an internal control (IC_{50} = 23 nM; K_B = 2.1 nM). Results are expressed as a percent inhibition of control agonist response. IC_{50} values were determined by non-linear regression of normalized response curves, using GraphPad Prism 6.0 software.

Small Animal PET-CT Imaging and Biodistribution Studies on the AsPC-1 Tumor Model. Animal experiments were conducted in compliance with the French laws, in application of the directive 2010/63/ EU and were approved by the "Charles Darwin" Institutional Animal Care and Use Committee of Sorbonne University #13184. AsPC1 tumor bearing mice (10 weeks old, 5×10^6 cells per mouse injected subcutaneously on the right shoulder in a 1:1 mixture of PBS and matrigel (BD Biosciences)) were intravenously (retro-orbitary sinus) injected with 4−6 MBq of a radiotracer (619 ± 36 pmol). Whole body static PET/computed tomography (CT) scans were performed under general anesthesia in a NanoScan PET/CT (Mediso Medical Imaging Systems Ltd., Budapest, Hungary) 50 or 90 min after injection during 20 min scans using multiple bed (three mice simultaneously). Anesthesia was induced and maintained during imaging by the administration of a mixture of isoflurane (1.5−2.5%) and oxygen. CT acquisitions were performed before PET acquisitions using the same bed position. PET and CT files were fused and converted to standardized uptake value (SUV) images using Nucline 2.03 Software (Mediso Medical Imaging Systems, Hungary). Images are analyzed and presented as coronal or axial slices. *Ex vivo* biodistribution was measured for n = 4 mice at 120 min post-injection (p.i.). Organs were collected, weighed, and γ-counted (Packard Instrument). Tumor or tissue uptakes are expressed as mean ± SD percentage injected dose per gram (%ID/g), corrected for radionuclide decay.

■ ASSOCIATED CONTENT

Supporting Information

The Supporting Information is available free of charge at https://pubs.acs.org/doi/10.1021/acs.jmedchem.1c00523.

Materials and general procedures, synthesis schemes, and analytical data for all compounds, *in vitro* stability data, *in vitro* binding affinity data, radiolabeling data, PET-MRI images, PET-CT images, tables of *ex vivo* biodistribution data determined by γ-counting, and blocking experiment data (PDF)

Animated 3D PET images (MP4)

SMILES formula of each compound and associated biochemical data (CSV)

■ AUTHOR INFORMATION

Corresponding Author

Victor Goncalves − *Institut de Chimie Moléculaire de l'Université de Bourgogne, ICMUB UMR CNRS 6302, Université Bourgogne Franche-Comté, Dijon 21000, France;* orcid.org/0000-0001-9854-4409; Email: victor.goncalves@u-bourgogne.fr

Authors

Emma Renard − *Institut de Chimie Moléculaire de l'Université de Bourgogne, ICMUB UMR CNRS 6302, Université Bourgogne Franche-Comté, Dijon 21000, France*

Mathieu Moreau − *Institut de Chimie Moléculaire de l'Université de Bourgogne, ICMUB UMR CNRS 6302, Université Bourgogne Franche-Comté, Dijon 21000, France*

Pierre-Simon Bellaye − *Georges-François LECLERC Cancer Center - UNICANCER, Dijon 21000, France*

Mélanie Guillemin − *Georges-François LECLERC Cancer Center - UNICANCER, Dijon 21000, France*

Bertrand Collin − *Georges-François LECLERC Cancer Center - UNICANCER, Dijon 21000, France*

Aurélie Prignon − *UMS28 Laboratoire d'Imagerie Moléculaire Positonique (LIMP), Sorbonne Université, Paris 75020, France;* orcid.org/0000-0002-3963-863X

Franck Denat − *Institut de Chimie Moléculaire de l'Université de Bourgogne, ICMUB UMR CNRS 6302, Université Bourgogne Franche-Comté, Dijon 21000, France*

Complete contact information is available at: https://pubs.acs.org/10.1021/acs.jmedchem.1c00523

Author Contributions

All authors have given approval to the final version of the manuscript.

Notes

The authors declare no competing financial interest.

■ ACKNOWLEDGMENTS

The authors thank the Plateforme d'Analyse Chimique et de Synthèse Moléculaire de l'Université de Bourgogne (http://www.wpcm.fr) for access to analytical instrumentation (specially Dr. M. Laly for the ionic chromatography and Dr. Q. Bonnin for the HRMS analysis). This work was partly funded by the French National Research Agency (ANR) under the French Investissements d'Avenir programs Equipex (IMAPPI, ANR-10-EQPX-05-01), AAP Générique 2017 (ZINELABEL, ANR-17-CE18-0016), and France Life Imaging (ANR-11-INBS-0006). This work was also supported by the CNRS and the Université de Bourgogne. This work is part of the project Pharmacoimagerie et agents théranostiques funded by the Conseil Régional de Bourgogne Franche-Comté through the Plan d'Action Régional pour l'Innovation (PARI) and by the European Union through the PO FEDER-FSE 2014/2020 Bourgogne program.

■ ABBREVIATIONS

CHO, Chinese hamster ovary; DOTA, 1,4,7,10-tetraazacyclododecane-1,4,7,10-tetraacetic acid; DOTAGA, 1,4,7,10-tetraazacyclododecane-1-glutaric acid-4,7,10-triacetic acid; NCS, *N*-chlorosuccinimide; NHS, *N*-hydroxysuccinimide; NOTA, 1,4,7-triazacyclononane-1,4,7-triacetic acid; NODAGA, 1,4,7-triazacyclononane-1-glutaric acid-4,7-diacetic acid; NTS1, neurotensin receptor 1; PBS, phosphate-buffered saline; PET, positron emission tomography; RP-HPLC, reversed-phase high-performance liquid chromatography; RT, room temperature; SD, standard deviation

■ REFERENCES

(1) Vaquero, J. J.; Kinahan, P. Positron Emission Tomography: Current Challenges and Opportunities for Technological Advances in Clinical and Preclinical Imaging Systems. *Annu. Rev. Biomed. Eng.* **2015**, *17*, 385−414.

(2) Wu, Z.; Martinez-Fong, D.; Trédaniel, J.; Forgez, P. Neurotensin and Its High Affinity Receptor 1 as a Potential Pharmacological Target in Cancer Therapy. *Front. Endocrinol.* **2013**, *3*, 184.

(3) Carraway, R. E.; Plona, A. M. Involvement of Neurotensin in Cancer Growth: Evidence, Mechanisms and Development of Diagnostic Tools. *Peptides* **2006**, *27*, 2445−2460.
(4) Reubi, J. C.; Waser, B.; Friess, H.; Buchler, M.; Laissue, J. Neurotensin Receptors: A New Marker for Human Ductal Pancreatic Adenocarcinoma. *Gut* **1998**, *42*, 546−550.
(5) Seethalakshmi, L.; Mitra, S. P.; Dobner, P. R.; Menon, M.; Carraway, R. E. Neurotensin Receptor Expression in Prostate Cancer Cell Line and Growth Effect of NT at Physiological Concentrations. *The Prostate* **1997**, *31*, 183−192.
(6) Reubi, J. C.; Waser, B.; Schaer, J. C.; Laissue, J. A. Neurotensin Receptors in Human Neoplasms: High Incidence in Ewing's Sarcomas. *Int. J. Cancer* **1999**, *82*, 213−218.
(7) Maoret, J. J.; Pospaï, D.; Rouyer-Fessard, C.; Couvineau, A.; Laboisse, C.; Voisin, T.; Laburthe, M. Neurotensin Receptor and Its MRNA Are Expressed in Many Human Colon Cancer Cell Lines but Not in Normal Colonic Epithelium: Binding Studies and RT-PCR Experiments. *Biochem. Biophys. Res. Commun.* **1994**, *203*, 465−471.
(8) Souazé, F.; Dupouy, S.; Viardot-Foucault, V.; Bruyneel, E.; Attoub, S.; Gespach, C.; Gompel, A.; Forgez, P. Expression of Neurotensin and NT1 Receptor in Human Breast Cancer: A Potential Role in Tumor Progression. *Cancer Res.* **2006**, *66*, 6243−6249.
(9) Reeve, J. G.; Goedert, M.; Emson, P. C.; Bleehen, N. M. Neurotensin in Human Small Cell Lung Carcinoma. *Recent Results Cancer Res.* **1985**, *99*, 175−176.
(10) Carraway, R.; Leeman, S. E. The Isolation of a New Hypotensive Peptide, Neurotensin, from Bovine Hypothalami. *J. Biol. Chem.* **1973**, *248*, 6854−6861.
(11) Prignon, A.; Provost, C.; Alshoukr, F.; Wendum, D.; Couvelard, A.; Barbet, J.; Forgez, P.; Talbot, J.-N.; Gruaz-Guyon, A. Preclinical Evaluation of 68Ga-DOTA-NT-20.3: A Promising PET Imaging Probe To Discriminate Human Pancreatic Ductal Adenocarcinoma from Pancreatitis. *Mol. Pharmaceutics* **2019**, *16*, 2776−2784.
(12) Maschauer, S.; Prante, O. Radiopharmaceuticals for Imaging and Endoradiotherapy of Neurotensin Receptor-Positive Tumors. *J. Labelled Compd. Radiopharm.* **2018**, *61*, 309−325.
(13) Yin, X.; Wang, M.; Wang, H.; Deng, H.; He, T.; Tan, Y.; Zhu, Z.; Wu, Z.; Hu, S.; Li, Z. Evaluation of Neurotensin Receptor 1 as a Potential Imaging Target in Pancreatic Ductal Adenocarcinoma. *Amino Acids* **2017**, *49*, 1325−1335.
(14) Renard, E.; Dancer, P.-A.; Portal, C.; Denat, F.; Prignon, A.; Goncalves, V. Design of Bimodal Ligands of Neurotensin Receptor 1 for Positron Emission Tomography Imaging and Fluorescence-Guided Surgery of Pancreatic Cancer. *J. Med. Chem.* **2020**, *63*, 2426−2433.
(15) Kitabgi, P.; De Nadai, F.; Rovère, C.; Bidard, J.-N. Biosynthesis, Maturation, Release, and Degradation of Neurotensin and Neuromedin N. *Ann. N. Y. Acad. Sci.* **1992**, *668*, 30−42.
(16) Gabriel, M.; Decristoforo, C.; Wöll, E.; Eisterer, W.; Nock, B.; Maina, T.; Moncayo, R.; Virgolini, I. [99mTc]Demotensin VI: Biodistribution and Initial Clinical Results in Tumor Patients of a Pilot/Phase I Study. *Cancer Biother. Radiopharm.* **2011**, *26*, 557−563.
(17) Gully, D.; Canton, M.; Boigegrain, R.; Jeanjean, F.; Molimard, J. C.; Poncelet, M.; Gueudet, C.; Heaulme, M.; Leyris, R.; Brouard, A. Biochemical and Pharmacological Profile of a Potent and Selective Nonpeptide Antagonist of the Neurotensin Receptor. *Proc. Natl. Acad. Sci. U. S. A.* **1993**, *90*, 65−69.
(18) Myers, R. M.; Shearman, J. W.; Kitching, M. O.; Ramos-Montoya, A.; Neal, D. E.; Ley, S. V. Cancer, Chemistry, and the Cell: Molecules That Interact with the Neurotensin Receptors. *ACS Chem. Biol.* **2009**, *4*, 503−525.
(19) Gully, D.; Labeeuw, B.; Boigegrain, R.; Oury-Donat, F.; Bachy, A.; Poncelet, M.; Pecceu, F.; Maffrand, J. P. Biochemical and Pharmacological Activities of SR 142948A, a New Potent Neurotensin Receptor Antagonist. *J. Pharmacol. Exp. Ther.* **1997**, *280*, 802−812.
(20) Betancur, C.; Canton, M.; Burgos, A.; Labeeuw, B.; Gully, D.; Rostene, W.; Pelaprata, D. Characterization of Binding Sites of a New Neurotensin Receptor Antagonist, [3H]SR 142948A, in the Rat Brain. *Eur. J. Pharmacol.* **1998**, *343*, 67−77.
(21) Lang, C.; Maschauer, S.; Hübner, H.; Gmeiner, P.; Prante, O. Synthesis and Evaluation of a ^{18}F-Labeled Diarylpyrazole Glycoconjugate for the Imaging of NTS1-Positive Tumors. *J. Med. Chem.* **2013**, *56*, 9361−9365.
(22) Schulz, J.; Rohracker, M.; Stiebler, M.; Goldschmidt, J.; Stöber, F.; Noriega, M.; Pethe, A.; Lukas, M.; Osterkamp, F.; Reineke, U.; Höhne, A.; Smerling, C.; Amthauer, H. Proof of Therapeutic Efficacy of a ^{177}Lu-Labeled Neurotensin Receptor 1 Antagonist in a Colon Carcinoma Xenograft Model. *J. Nucl. Med.* **2017**, *58*, 936−941.
(23) Ginj, M.; Zhang, H.; Waser, B.; Cescato, R.; Wild, D.; Wang, X.; Erchegyi, J.; Rivier, J.; Mäcke, H. R.; Reubi, J. C. Radiolabeled Somatostatin Receptor Antagonists Are Preferable to Agonists for in Vivo Peptide Receptor Targeting of Tumors. *Proc. Natl. Acad. Sci. U. S. A.* **2006**, *103*, 16436−16441.
(24) Fani, M.; Maecke, H. R. Radiopharmaceutical Development of Radiolabelled Peptides. *Eur. J. Nucl. Med. Mol. Imaging* **2012**, *39*, 11−30.
(25) Dash, A.; Chakraborty, S.; Pillai, M. R. A.; Knapp, F. F. R., Jr. Peptide Receptor Radionuclide Therapy: An Overview. *Cancer Biother. Radiopharm.* **2015**, *30*, 47−71.
(26) Schulz, J.; Rohracker, M.; Stiebler, M.; Goldschmidt, J.; Grosser, O. S.; Osterkamp, F.; Pethe, A.; Reineke, U.; Smerling, C.; Amthauer, H. Comparative Evaluation of the Biodistribution Profiles of a Series of Nonpeptidic Neurotensin Receptor-1 Antagonists Reveals a Promising Candidate for Theranostic Applications. *J. Nucl. Med.* **2016**, *57*, 1120−1123.
(27) *Study to Evaluate the Safety and Activity (Including Distribution) of 177Lu-3BP-227 in Subjects With Solid Tumours Expressing Neurotensin Receptor Type 1. - Tabular View - ClinicalTrials.gov*. https://clinicaltrials.gov/ct2/show/record/NCT03525392, (accessed Apr 23, 2020).
(28) Baum, R. P.; Singh, A.; Schuchardt, C.; Kulkarni, H. R.; Klette, I.; Wiessalla, S.; Osterkamp, F.; Reineke, U.; Smerling, C. ^{177}Lu-3BP-227 for Neurotensin Receptor 1−Targeted Therapy of Metastatic Pancreatic Adenocarcinoma: First Clinical Results. *J. Nucl. Med.* **2018**, *59*, 809−814.
(29) Ametamey, S. M.; Honer, M.; Schubiger, P. A. Molecular Imaging with PET. *Chem. Rev.* **2008**, *108*, 1501−1516.
(30) Brandt, M.; Cardinale, J.; Aulsebrook, M. L.; Gasser, G.; Mindt, T. L. An Overview of PET Radiochemistry, Part 2: Radiometals. *J. Nucl. Med.* **2018**, *59*, 1500−1506.
(31) International Atomic Energy Agency. *Gallium-68 Cyclotron Production; TECDOC Series*; International Atomic Energy Agency: Vienna, 2019.
(32) Price, E. W.; Orvig, C. Matching Chelators to Radiometals for Radiopharmaceuticals. *Chem. Soc. Rev.* **2014**, *43*, 260−290.
(33) Spang, P.; Herrmann, C.; Roesch, F. Bifunctional Gallium-68 Chelators: Past, Present, and Future. *Seminars in Nuclear Medicine* **2016**, *46*, 373−394.
(34) Tsionou, M. I.; Knapp, C. E.; Foley, C. A.; Munteanu, C. R.; Cakebread, A.; Imberti, C.; Eykyn, T. R.; Young, J. D.; Paterson, B. M.; Blower, P. J.; Ma, M. T. Comparison of Macrocyclic and Acyclic Chelators for Gallium-68 Radiolabelling. *RSC Adv.* **2017**, *7*, 49586−49599.
(35) Malmberg, J.; Perols, A.; Varasteh, Z.; Altai, M.; Braun, A.; Sandström, M.; Garske, U.; Tolmachev, V.; Orlova, A.; Karlström, A. E. Comparative Evaluation of Synthetic Anti-HER2 Affibody Molecules Site-Specifically Labelled with 111In Using N-Terminal DOTA, NOTA and NODAGA Chelators in Mice Bearing Prostate Cancer Xenografts. *Eur. J. Nucl. Med. Mol. Imaging* **2012**, *39*, 481−492.
(36) Mitran, B.; Varasteh, Z.; Selvaraju, R. K.; Lindeberg, G.; Sörensen, J.; Larhed, M.; Tolmachev, V.; Rosenström, U.; Orlova, A. Selection of Optimal Chelator Improves the Contrast of GRPR Imaging Using Bombesin Analogue RM26. *Int. J. Oncol.* **2016**, *48*, 2124−2134.
(37) Mitran, B.; Thisgaard, H.; Rinne, S.; Dam, J. H.; Azami, F.; Tolmachev, V.; Orlova, A.; Rosenström, U. Selection of an Optimal Macrocyclic Chelator Improves the Imaging of Prostate Cancer Using Cobalt-Labeled GRPR Antagonist RM26. *Sci. Rep.* **2019**, *9*, 17086.
(38) Rinne, S. S.; Dahlsson Leitao, C.; Gentry, J.; Mitran, B.; Abouzayed, A.; Tolmachev, V.; Ståhl, S.; Löfblom, J.; Orlova, A.

Increase in Negative Charge of 68Ga/Chelator Complex Reduces Unspecific Hepatic Uptake but Does Not Improve Imaging Properties of HER3-Targeting Affibody Molecules. *Sci. Rep.* **2019**, *9*, 17710.
(39) Rinne, S. S.; Leitao, C. D.; Mitran, B.; Bass, T. Z.; Andersson, K. G.; Tolmachev, V.; Ståhl, S.; Löfblom, J.; Orlova, A. Optimization of HER3 Expression Imaging Using Affibody Molecules: Influence of Chelator for Labeling with Indium-111. *Sci. Rep.* **2019**, *9*, 655.
(40) Varasteh, Z.; Mitran, B.; Rosenström, U.; Velikyan, I.; Rosestedt, M.; Lindeberg, G.; Sörensen, J.; Larhed, M.; Tolmachev, V.; Orlova, A. The Effect of Macrocyclic Chelators on the Targeting Properties of the 68Ga-Labeled Gastrin Releasing Peptide Receptor Antagonist PEG2-RM26. *Nucl. Med. Biol.* **2015**, *42*, 446−454.
(41) Roxin, Á.; Zhang, C.; Huh, S.; Lepage, M.; Zhang, Z.; Lin, K.-S.; Bénard, F.; Perrin, D. M. A Metal-Free DOTA-Conjugated ^{18}F-Labeled Radiotracer: [^{18}F]DOTA-AMBF$_3$-LLP2A for Imaging VLA-4 Over-Expression in Murine Melanoma with Improved Tumor Uptake and Greatly Enhanced Renal Clearance. *Bioconjugate Chem.* **2019**, *30*, 1210−1219.
(42) Labeeuw, B.; Gully, D.; Jeanjean, F.; Molimard, J.-C.; Boigegrain, R. Manufacturing method of semiconductor device. Patent JP5723483B2. 1998, 58.
(43) Baxendale, I. R.; Cheung, S.; Kitching, M. O.; Ley, S. V.; Shearman, J. W. The Synthesis of Neurotensin Antagonist SR 48692 for Prostate Cancer Research. *Bioorg. Med. Chem.* **2013**, *21*, 4378−4387.
(44) Kurosawa, W.; Kan, T.; Fukuyama, T. Preparation of Secondary Amines from Primary Amines via 2-Nitrobenzenesulfonamides: N-(4-Methoxybenzyl)-3-Phenylpropylamine. *Org. Synth.* **2002**, *79*, 186.
(45) Battilocchio, C.; Baxendale, I. R.; Biava, M.; Kitching, M. O.; Ley, S. V. A Flow-Based Synthesis of 2-Aminoadamantane-2-Carboxylic Acid. *Org. Process Res. Dev.* **2012**, *16*, 798−810.
(46) Battilocchio, C.; Deadman, B. J.; Nikbin, N.; Kitching, M. O.; Baxendale, I. R.; Ley, S. V. A Machine-Assisted Flow Synthesis of SR48692: A Probe for the Investigation of Neurotensin Receptor-1. *Chem. − Eur. J.* **2013**, *19*, 7917−7930.
(47) Lang, C.; Gmeiner, P. Efficient Synthesis of Heterocyclic Neurotensin Receptor Ligands by Microwave-Assisted Aminocarbonylation. *Synthesis* **2013**, *45*, 2474−2480.
(48) Price, T. W.; Greenman, J.; Stasiuk, G. J. Current Advances in Ligand Design for Inorganic Positron Emission Tomography Tracers 68Ga, 64Cu, 89Zr and 44Sc. *Dalton Trans.* **2016**, *45*, 15702−15724.
(49) Vita, N.; Laurent, P.; Lefort, S.; Chalon, P.; Dumont, X.; Kaghad, M.; Gully, D.; Le Fur, G.; Ferrara, P.; Caput, D. Cloning and Expression of a Complementary DNA Encoding a High Affinity Human Neurotensin Receptor. *FEBS Lett.* **1993**, *317*, 139−142.
(50) Andrés, A.; Rosés, M.; Ràfols, C.; Bosch, E.; Espinosa, S.; Segarra, V.; Huerta, J. M. Setup and Validation of Shake-Flask Procedures for the Determination of Partition Coefficients (LogD) from Low Drug Amounts. *Eur. J. Pharm. Sci.* **2015**, *76*, 181−191.
(51) Alshoukr, F.; Rosant, C.; Maes, V.; Abdelhak, J.; Raguin, O.; Burg, S.; Sarda, L.; Barbet, J.; Tourwé, D.; Pelaprat, D.; Gruaz-Guyon, A. Novel Neurotensin Analogues for Radioisotope Targeting to Neurotensin Receptor-Positive Tumors. *Bioconjugate Chem.* **2009**, *20*, 1602−1610.
(52) Alshoukr, F.; Prignon, A.; Brans, L.; Jallane, A.; Mendes, S.; Talbot, J.-N.; Tourwé, D.; Barbet, J.; Gruaz-Guyon, A. Novel DOTA-Neurotensin Analogues for 111In Scintigraphy and 68Ga PET Imaging of Neurotensin Receptor-Positive Tumors. *Bioconjugate Chem.* **2011**, *22*, 1374−1385.
(53) Hosseinimehr, S. J.; Tolmachev, V.; Orlova, A. Liver Uptake of Radiolabeled Targeting Proteins and Peptides: Considerations for Targeting Peptide Conjugate Design. *Drug Discovery Today* **2012**, *17*, 1224−1232.
(54) Hodolic, M.; Wu, W. Y.; Zhao, Z.; Yu, F.; Virgolini, I.; Wang, F. Safety and Tolerability of 68Ga-NT-20.3, a Radiopharmaceutical for Targeting Neurotensin Receptors, in Patients with Pancreatic Ductal Adenocarcinoma: The First in-Human Use. *Eur. J. Nucl. Med.* **2021**, 1229.
(55) Buchegger, F.; Bonvin, F.; Kosinski, M.; Schaffland, A. O.; Prior, J.; Reubi, J. C.; Bläuenstein, P.; Tourwé, D.; García Garayoa, E.; Bischof Delaloye, A. Radiolabeled Neurotensin Analog, 99mTc-NT-XI, Evaluated in Ductal Pancreatic Adenocarcinoma Patients. *J. Nucl. Med.* **2003**, *44*, 1649−1654.
(56) Fani, M.; Del Pozzo, L.; Abiraj, K.; Mansi, R.; Tamma, M. L.; Cescato, R.; Waser, B.; Weber, W. A.; Reubi, J. C.; Maecke, H. R. PET of Somatostatin Receptor-Positive Tumors Using 64Cu- and 68Ga-Somatostatin Antagonists: The Chelate Makes the Difference. *J. Nucl. Med.* **2011**, *52*, 1110−1118.
(57) Banerjee, S. R.; Chen, Z.; Pullambhatla, M.; Lisok, A.; Chen, J.; Mease, R. C.; Pomper, M. G. Preclinical Comparative Study of 68Ga-Labeled DOTA, NOTA, and HBED-CC Chelated Radiotracers for Targeting PSMA. *Bioconjugate Chem.* **2016**, *27*, 1447−1455.
(58) Roosenburg, S.; Laverman, P.; Joosten, L.; Cooper, M. S.; Kolenc-Peitl, P. K.; Foster, J. M.; Hudson, C.; Leyton, J.; Burnet, J.; Oyen, W. J. G.; Blower, P. J.; Mather, S. J.; Boerman, O. C.; Sosabowski, J. K. PET and SPECT Imaging of a Radiolabeled Minigastrin Analogue Conjugated with DOTA, NOTA, and NODAGA and Labeled with (64)Cu, (68)Ga, and (111)In. *Mol. Pharmaceutics* **2014**, *11*, 3930−3937.
(59) Leitao, C. D.; Rinne, S. S.; Mitran, B.; Vorobyeva, A.; Andersson, K. G.; Tolmachev, V.; Ståhl, S.; Löfblom, J.; Orlova, A. Molecular Design of HER3-Targeting Affibody Molecules: Influence of Chelator and Presence of HEHEHE-Tag on Biodistribution of 68Ga-Labeled Tracers. *Int. J. Mol. Sci.* **2019**, *20*, 1080.
(60) von Witting, E.; Garousi, J.; Lindbo, S.; Vorobyeva, A.; Altai, M.; Oroujeni, M.; Mitran, B.; Orlova, A.; Hober, S.; Tolmachev, V. Selection of the Optimal Macrocyclic Chelators for Labeling with 111In and 68Ga Improves Contrast of HER2 Imaging Using Engineered Scaffold Protein ADAPT6. *Eur. J. Pharm. Biopharm.* **2019**, *140*, 109−120.
(61) Lin, M.; Welch, M. J.; Lapi, S. E. Effects of Chelator Modifications on 68Ga-Labeled [Tyr3]Octreotide Conjugates. *Mol. Imaging Biol.* **2013**, *15*, 606−613.
(62) Young, J. D.; Abbate, V.; Imberti, C.; Meszaros, L. K.; Ma, M. T.; Terry, S. Y. A.; Hider, R. C.; Mullen, G. E.; Blower, P. J. 68Ga-THP-PSMA: A PET Imaging Agent for Prostate Cancer Offering Rapid, Room-Temperature, 1-Step Kit-Based Radiolabeling. *J. Nucl. Med.* **2017**, *58*, 1270−1277.
(63) Fanelli, R.; Chastel, A.; Previti, S.; Hindié, E.; Vimont, D.; Zanotti-Fregonara, P.; Fernandez, P.; Garrigue, P.; Lamare, F.; Schollhammer, R.; Balasse, L.; Guillet, B.; Rémond, E.; Morgat, C.; Cavelier, F. Silicon-Containing Neurotensin Analogues as Radiopharmaceuticals for NTS(1)-Positive Tumors Imaging. *Bioconjugate Chem.* **2020**, *31*, 2339−2349.

https://doi.org/10.1021/acs.jmedchem.1c00523
J. Med. Chem. 2021, 64, 8564−8578